

# 000 001 002 003 004 005 TIR-BENCH: A COMPREHENSIVE BENCHMARK FOR 006 AGENTIC THINKING-WITH-IMAGES REASONING 007 008 009

010 **Anonymous authors**  
011 Paper under double-blind review  
012  
013  
014  
015  
016  
017  
018  
019  
020  
021  
022  
023

## ABSTRACT

024  
025 The frontier of visual reasoning is shifting toward models like OpenAI o3, which  
026 can intelligently create and operate tools to transform images for problem-solving,  
027 also known as thinking-*with*-images in chain-of-thought. Yet existing benchmarks  
028 fail to fully capture this advanced capability. Even Visual Search, the most com-  
029 mon benchmark for current thinking-*with*-images methods, tests only basic oper-  
030 ations such as localization and cropping, offering little insight into more complex,  
031 dynamic, and tool-dependent reasoning. We introduce **TIR-Bench**, a com-  
032 prehensive benchmark for evaluating agentic thinking-*with*-images across 13 diverse  
033 tasks, each requiring novel tool use for image processing and manipulation in  
034 chain-of-thought. We evaluate 22 multimodal large language models (MLLMs),  
035 from leading open-sourced and proprietary models to those with explicit tool-  
036 use augmentation. Results show that TIR-Bench is universally challenging, and  
037 strong performance requires genuine thinking-*with*-images capabilities. Finally,  
038 we present a pilot study comparing direct versus agentic fine-tuning.  
039

## 1 INTRODUCTION

040 The reasoning abilities of recent multimodal large language models (MLLMs) (Hurst & OpenAI,  
041 2024; Gemini Team, 2025) have advanced significantly, driven in large part by reasoning techniques  
042 such as chain-of-thought (CoT) (Wei et al., 2022). By decomposing reasoning of complex visual  
043 questions into a series of textual steps, MLLMs are able to achieve improved performance. While  
044 promising, these techniques are confined to the textual domain, conducting their reasoning solely  
045 through language while treating the visual information as a static, unalterable input (Su et al., 2025b).  
046

047 To effectively process visual information, thinking-*with*-images has been proposed (OpenAI, 2025c;  
048 Su et al., 2025b; Hu et al., 2024). This approach enables a model to generate new visual information  
049 by actively manipulating input images with tools. For example, when faced with a complex visual  
050 problem, OpenAI’s o3 model (OpenAI, 2025c) first writes code to create an image-processing tool,  
051 then executes it to modify the image (e.g., cropping, flipping, or rotating). The transformed visual  
052 data then informs the next stage of its linguistic reasoning.  
053

054 To assess the agentic thinking-*with*-images capabilities of MLLMs, existing benchmarks (Wu &  
055 Xie, 2024; Wang et al., 2025) have largely centered on visual search and tasks requiring the analysis  
056 of high-resolution images. These evaluations primarily validate a model’s ability to accurately lo-  
057 calize and crop specific regions within an image for better capturing detailed information to answer  
058 corresponding questions. However, these assessments tend to focus narrowly on the visual search  
059 capabilities of agentic MLLMs, leaving a broader spectrum of thinking-*with*-images abilities un-  
060 evaluated. Therefore, there is an urgent need for a benchmark that incorporates a diverse range of  
061 tasks requiring sophisticated tool use to properly assess integrated multimodal reasoning.  
062

063 In this paper, we introduce TIR-Bench, a comprehensive benchmark designed to evaluate the diverse  
064 thinking-*with*-images capabilities of agentic MLLMs. Unlike previous benchmarks focusing solely  
065 on visual search problems, TIR-Bench incorporates a diverse set of 13 tasks that require a wide range  
066 of tool-based interactions, such as zooming, rotating, increasing image contrast, adding auxiliary  
067 lines, and others to assess a model’s tool integrated reasoning capabilities. The design of each task  
068 is predicated on the human intuition that solving it requires actively manipulating the visual input,  
069 rather than relying on static observation alone. For example, in TIR-Bench, a math problem might  
070 require the model to draw auxiliary lines or a coordinate system to find a solution, while a jigsaw  
071

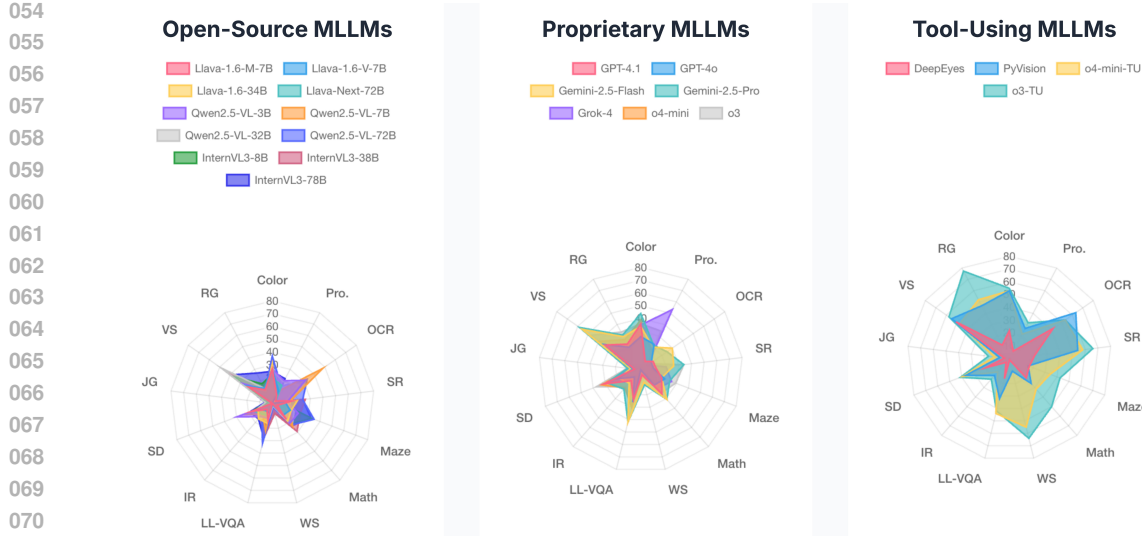


Figure 1: Overview of performance of open models (left), proprietary models (middle), and agentic tool-using models (right). SR: Symbolic Reasoning, WS: Word Search, LL-VQA: Low-Light VQA, IR: Instrument Reasoning, SD: Spot Difference, JG: Jigsaw Game, VS: Visual Search, RG: Rotation Game, Pro.: Proportion VQA. o3-TU: o3-tool-using, i.e., o3 with code interpreter.

puzzle task demands that it segment and then reassemble the image pieces. Consequently, TIR-Bench enables a more holistic evaluation of a model’s thinking-with-images abilities, assessing a spectrum of skills not limited to visual search.

Using TIR-Bench, we conduct a comprehensive performance evaluation of 22 leading MLLMs across three categories: open-source models, proprietary models, and tool-using agents. The overall experimental results, illustrated in Figure 1, reveal that TIR-Bench is a challenging benchmark for thinking-with-images abilities, as the best performance achieved is only 46%. Moreover, traditional non-agentic models perform poorly on TIR-Bench, with the best-performing model Gemini-2.5-pro reaching an accuracy of merely 28.9%. These findings highlight the importance of the thinking-with-images ability for this benchmark, as models equipped with tool-use capabilities, such as o3, o4-mini, and PyVision (Zhao et al., 2025), achieve much higher performance than other models.

Lastly, we assess the function-calling proficiency of various MLLMs and conduct a pilot study contrasting direct supervised fine-tuning (SFT) with an agentic SFT approach on rotated image OCR task. Many recent MLLMs are equipped with function-calling capabilities. Our evaluation on rotation game task of TIR-Bench measures a model’s proficiency in accurately executing the correct tool parameters as part of its reasoning chain. Results show that recent models like o3 perform well, whereas earlier models such as GPT-4o perform significantly worse. The pilot study on the rotated image OCR task compares two training methodologies and examines whether end-to-end SFT can achieve strong performance across different data scales for tasks involving image operations. Our findings indicate that the agentic SFT on full problem-solving trajectories with generated images is significantly more effective than direct SFT on rotated OCR task. This implies that agentic fine-tuning enables the emergence of more complex and robust problem-solving behaviors, allowing models to tackle multi-step tasks that are intractable with direct fine-tuning alone.

## 2 RELATED WORKS

### 2.1 MULTIMODAL BENCHMARKS

As the capabilities of Multimodal Large Language Models (MLLMs) evolve rapidly, a variety of benchmarks have been proposed to evaluate their performance, identify limitations, and guide future improvements (Lu et al., 2023; Zhang et al., 2024; Qiao et al., 2024; Wang et al., 2024a;b; Li et al., 2024c; Lu et al., 2021; Li et al., 2025). These benchmarks are typically either specialized for specific domains (Wang et al., 2024b; Li et al., 2024c; Lu et al., 2021; Li et al., 2025) or designed to be versatile and cover a broad range of tasks (Li et al., 2024b; Liu et al., 2023; Yue et al.,

2024; Wang et al., 2023). MLLMs often use CoT reasoning on these benchmarks, though solving them only requires static image information. More recently, benchmarks such as V\* Bench and HR-Bench have been introduced to evaluate agentic capabilities, specifically for visual search in high-resolution images (Wu & Xie, 2024; Wang et al., 2025). While these benchmarks advance agentic evaluation by requiring models to programmatically crop high-resolution images, their focus is narrowly confined to visual search. Consequently, a broader spectrum of thinking-with-images abilities, such as rotation and drawing, remains largely underexplored.

## 2.2 THINK WITH IMAGES

In previous works, Visual Sketchpad (Hu et al., 2024), CoGCoM (Qi et al., 2025), DeepEyes (Zheng et al., 2025), Pixel Reasoner (Su et al., 2025a), OpenThinkIMG (Su et al., 2025b), Chain-of-Focus (Zhang et al., 2025a), Mini-o3 (Lai et al., 2025) and REVPT (Zhou et al., 2025) generate and executes tool calling in a predefined visual-specific toolset. In the intermediate reasoning steps, processed images are reinjected to the context, resulting in a multi-modal rational. However, these methods rely on a fixed collection of external visual parsers—such as detection models (e.g., GroundingDINO (Liu et al., 2024b)) and segmentation models (e.g., SAM (Kirillov et al., 2023a))—which constrains their generality across diverse vision tasks and introduces bottlenecks due to dependency on external models. In contrast, ViperGPT (Surís et al., 2023), o3 (OpenAI, 2025a), o4-mini, Thyme (Zhang et al., 2025b) and PyVision (Zhao et al., 2025) adopt Python as its primitive tool. Capitalizing on the advanced coding and multimodal understanding capabilities of modern MLLMs—such as Claude-4.0 (Anthropic, 2025) and GPT-4.1 (OpenAI, 2025b), enables the MLLM to dynamically write and execute code to construct complex, task-specific tools on demand, thereby supporting more general and flexible reasoning. This aligns with the emerging paradigm of “thinking with images” highlighted in o3’s blog (OpenAI, 2025c) as a powerful cognitive capability. To assess this important ability, we propose TIR-Bench, covering diverse tasks on which multi-modal rationals are necessary.

## 3 TIR-BENCH

In this section, we introduce **TIR-Bench**. The overview of the benchmark is shown in Figure 2. We first introduce the task design strategy in subsection 3.1. Next, we introduce the data collection process in subsection 3.2. Finally, we present the benchmark summary in subsection 3.3.

### 3.1 TASK DESIGN

To extensively validate the model’s ability to think with images we design 13 tasks. The benchmark’s tasks are designed to evaluate a model’s ability to perform active, tool-based visual reasoning, moving far beyond static image analysis. This includes tasks that require programmatic analysis, such as calculating color proportions or calling external models for object segmentation. Other challenges test the model’s ability to overcome suboptimal conditions by programmatically enhancing low-light images or correcting the orientation of rotated text before performing OCR. The benchmark also features complex spatial and algorithmic puzzles, requiring models to solve mazes, reassemble jigsaw pieces, or draw auxiliary lines to solve geometric problems. Finally, it assesses fine-grained perception through tasks like spotting differences between images, reading instruments via cropping and zooming, and locating anomalies in visual puzzles. In every case, the model is forced to engage in a dynamic, multi-step process of visual manipulation and reasoning to arrive at the correct answer. More details about task design are introduced in Appendix B.

### 3.2 DATA COLLECTION

**Guidelines.** As previously mentioned, current benchmarks focus almost exclusively on visual search, overlooking a wide range of other tool-using abilities. To bridge this evaluation gap, we designed TIR-Bench in accordance with the following guidelines: (1) Diverse, Application-Grounded Tasks: TIR-Bench covers 13 distinct tasks across multiple domains, including spatial reasoning, visual perception, and mathematics, to mirror the complexity of real-world applications where static image analysis is insufficient. (2) Comprehensive Skill Assessment: The benchmark incorporates diverse visual contexts and requires a range of programmatic skills—from drawing auxiliary lines in

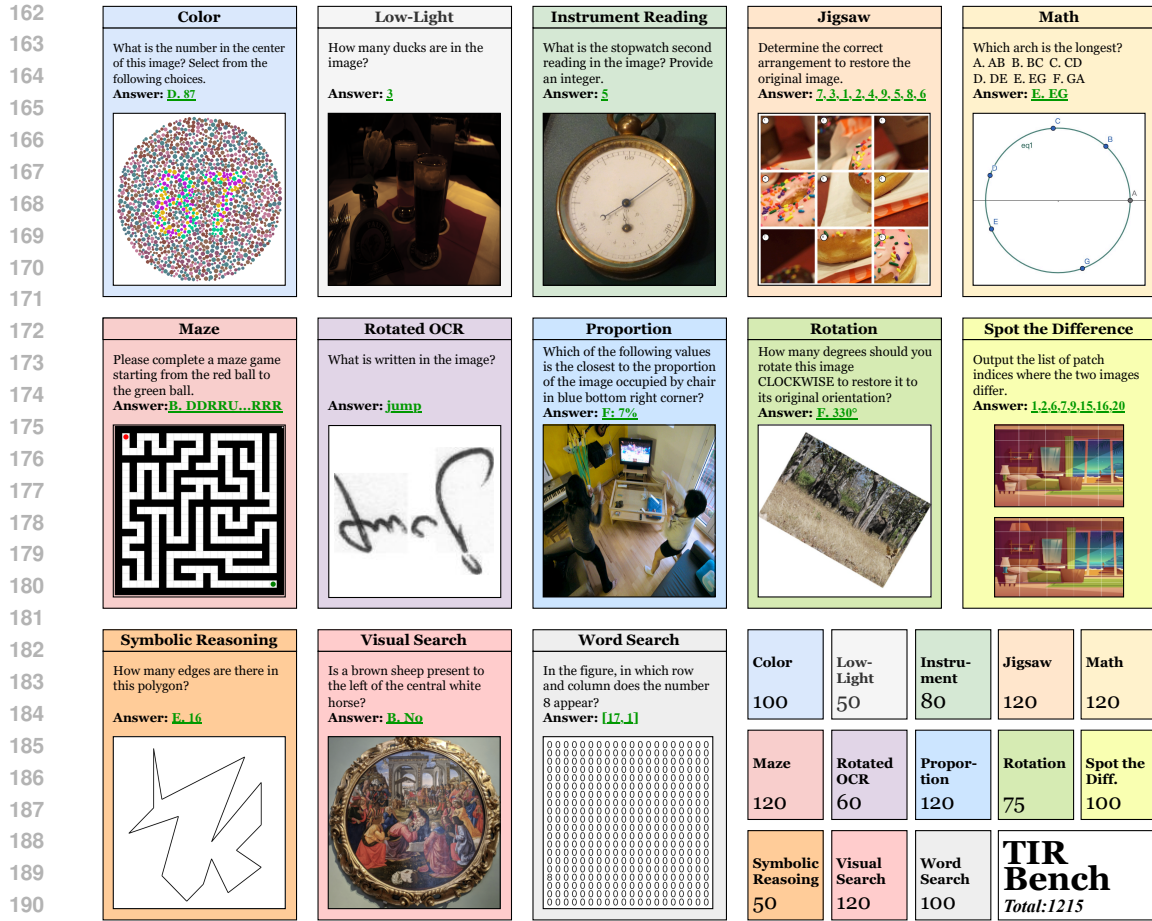


Figure 2: **Benchmark Overview.** TIR-Bench is composed of 13 tasks, meticulously designed to evaluate a wide spectrum of thinking-with-images capabilities.

geometry to executing pixel-level analysis—to foster a well-rounded evaluation of a model’s agentic capabilities. (3) Probing Model Limitations: Each task is designed to be unsolvable without a multi-step, tool-based strategy. This intentional difficulty probes the limitations of current models, effectively distinguishing true thinking-with-images reasoning from simpler visual recognition. (4) Deterministic Evaluation: all tasks are designed with objectively verifiable answers, providing a robust framework for deterministic and reproducible evaluations. (5) Many samples in TIR-Bench are newly annotated or generated, making it a more reliable benchmark that minimizes the risk of data contamination from models’ pre-training corpora.

**Collection.** We briefly introduce the data collection process of the 13 tasks here, while the detailed process can be found in Appendix B. The summary of data collection is shown in Table 1. Data from existing benchmarks are covered by the Apache License 2.0 or other licenses that permit academic use. For newly annotated data, images were sourced from freely available platforms like Wikimedia Commons and the National Gallery of Art, or were created by students using tools such as GeoGebra.

**(1). Collection of Math VQA, Symbolic Reasoning, Low-Light VQA, and Instrument Reading tasks:** Data from these tasks are newly created and annotated data. We tasked two Ph.D. students with sourcing free images from the Internet and MathVista (Lu et al., 2023) or create images using Geogebra, and then creating corresponding question-answer pairs. The annotators were explicitly instructed to design problems that, in their judgment, would necessitate tool-based image manipulation for a solution, ensuring the tasks could not be solved by static observation alone. Both students engaged in a reciprocal cross-checking process to verify the correctness of both the problems and their respective answers.

Attribute	Color VQA	Proportion VQA	Symbolic Reasoning		Math	Word Search	Rotated OCR
Image Source	ColorBench	RefCOCO	VlmsAreBlind + Web-sourced	Web-sourced	Web-sourced	OCRBenck	
QA Construction	Human-annotated	Synthetic	Human-annotated		Human-annotated	Synthetic	Dataset-provided
Samples	100	120	50		120	100	60
Answer Type	Single-choice	Single-choice	Single-choice		Single-choice	Open-ended	Open-ended

Attribute	Maze	Low-Light	Instrument Reading	Spot the Difference	Jigsaw	Visual Search	Rotation
Image Source	Synthetic	Web-sourced	Web-sourced	Web-sourced	Synthetic	Web-sourced	CVBench
QA Construction	Synthetic	Human-annotated	Human-annotated	Human-annotated	Synthetic	Synthetic	Synthetic
Samples	120	50	80	100	120	120	75
Answer Type	Single-choice	Open-ended	Open-ended	Open-ended	Open-ended	Single-choice	Single-choice

Table 1: Overview of all tasks, grouped into reasoning-oriented (top) and perception-oriented (bottom), with their sources, QA constructions, sample sizes, and answer types.

**(2). Collection of Color VQA task:** We tasked a Ph.D. student with curating samples from the ColorBench (Liang et al., 2025), specifically selecting instances that could not be solved by static observation alone and therefore necessitate programmatic analysis to answer correctly. Finally, we select 100 problems from ColorBench (Liang et al., 2025).

**(3). Collection of Jigsaw, Maze, Rotation, Word Search Tasks:** The data for these tasks were programmatically generated to create controlled and scalable challenges. For the Jigsaw Puzzle, we selected 120 images from the RefCOCO dataset, chosen for their prominent objects. These images were then segmented into grids ranging from  $3 \times 3$  to  $6 \times 6$  and shuffled to create puzzles of varying difficulty. For the Maze task, we programmatically generated 100 mazes with sizes scaling from  $5 \times 5$  to  $62 \times 62$ . For the Rotation Game, we utilized 75 images from CVBench (Tong et al., 2024), to which we applied random rotations. Three difficulty tiers were established based on the magnitude of the rotation angle (e.g., 5, 10, or 15 degrees). Finally, for the Word Search task, we programmatically generated 85 samples of different sizes and supplemented them with 15 complex puzzles sourced from the internet.

**(4). Collection of Spot the Difference:** We sourced pairs of nearly identical cartoon and real-world images from the internet, with one image in each pair containing subtle alterations. Both images were then segmented into an  $m \times n$  grid of corresponding patches. Finally, two annotators reviewed the pairs to identify and label the specific patches that contained the differences. Both students engaged in a reciprocal cross-checking process to verify the correctness of difference patch numbers.

**(5). Collection of Proportion VQA:** For this task, we collected 120 images from the RefCOCO dataset and used the ground-truth segmentation masks to calculate the correct object proportions. The incorrect multiple-choice options were then generated by adding or subtracting eight percentage points from the true value.

**(6). Collection of Rotated Image OCR Task:** We selected 60 images from OCRBenck and applied a rotation to each. The rotation probabilities were 25% for  $90^\circ$ , 25% for  $270^\circ$ , and 50% for  $180^\circ$ .

**(7). Collection of Visual Search:** Recognizing that problems in existing benchmarks like V\* Benck (Wu & Xie, 2024) are often too simple for current models, we curated a more challenging dataset for this task. We began by selecting 32 difficult problems from HR-Bench (Wang et al., 2025). To supplement these, we collected 88 new samples, which include 25 high-resolution art images and 63 high-resolution real-world images sourced from the internet. For each of these new images, an annotator was tasked with generating a unique question-answer pair. In total, the Visual Search task comprises 120 samples, 88 of which are newly created for this benchmark.

### 3.3 BENCHMARK SUMMARY

TIR-Benck consists of a total of 1215 examples divided into 13 diverse but essential tasks. Questions in our benchmark are categorized into two types: multi-choice and free-form problems, counting 665 and 550, respectively. The average length for question text is 46.29 and the average length for

270 answer text is 3.41. The distribution of each task is shown in Figure 7. Image and question examples  
 271 for each task are shown in Appendix C.  
 272

## 273 4 EXPERIMENTS

276 In this section, we detail our evaluation setup and results for 22 leading MLLMs, considering both  
 277 models with and without agentic tool-use capabilities. Our goal is to show that MLLMs lacking  
 278 the ability to think with images perform poorly on TIR-Bench. We describe the experimental setup  
 279 in subsection 4.1, report the results in subsection 4.2, present experiments on function calling in  
 280 subsection 4.4, and compare agentic SFT with end-to-end SFT in subsection 4.5.  
 281

### 282 4.1 EXPERIMENT SETUP

283 **Model selection.** We categorize the MLLMs we use into open-source, proprietary, and tool-using.  
 284 For open-sourced, we evaluated 11 models across three widely used and up-to-date model families:  
 285 DeepSeek-VL-2 Wu et al. (2024), Kwai Keye-VL Team et al. (2025), Phi-4-Multimodal Aboue-  
 286 lenin et al. (2025), LLaVA (Li et al., 2024a; Liu et al., 2024a), Qwen2.5-VL (Bai et al., 2025),  
 287 InternVL3 (Zhu et al., 2025), and Qwen3-VL Team (2025), ranging from 3B to 78B. Results from  
 288 these models accurately reflect open-source MLLMs’ performance on thinking-with-image reason-  
 289 ing tasks. For proprietary models, we selected 7 models across 3 model families: GPT (Hurst &  
 290 OpenAI, 2024), Gemini-2.5 (Gemini Team, 2025), and Grok-4 (xAI, 2025). We test GPT series,  
 291 including GPT-4.1, GPT-4o (Hurst & OpenAI, 2024), as well as o-series models (OpenAI, 2025a),  
 292 including o3 and o4-mini. For these GPT models, we use Azure API for calling models w/o python  
 293 interpreter or sandbox (OpenAI, 2025c). For agentic tool-using (TU) MLLMs, we evaluate three  
 294 open-sourced frameworks: DeepEyes (Zheng et al., 2025), and PyVision (Zhao et al., 2025), and  
 295 2 proprietary models o4-mini-TU and o3-TU. We use the official OpenAI API and turn on code  
 296 interpreter and set the container parameter as auto.  
 297

298 **Evaluation.** We follow previous works (Lu et al., 2023; Li et al., 2025) to first generate answers  
 299 from models and subsequently using GPT-4o to extract the final answer from the answer content.  
 300 For multiple-choice and short-form answers, we compare the extracted value directly against the  
 301 ground-truth to calculate accuracy; for grounding type problems such as Jigsaw Game and Spot the  
 302 Difference with list type answer, we calculate the intersection over union (IoU).  
 303

304 **Implementation details.** We conduct all evaluations in zero-shot manner for fair comparison and  
 305 better generalization. For open models, all experiments are done on NVIDIA A100 GPUs. For  
 306 proprietary models, we use the official API. More details can be found in the Appendix E.  
 307

### 308 4.2 EXPERIMENTAL RESULTS

309 Both average and task-wise accuracies are reported in Table 2. We discuss several findings below.  
 310

311 **Result 1: TIR-Bench is challenging for all model types.** The highest performance observed  
 312 among all models is only 46%, a result that underscores the difficulty of the TIR-Bench. This  
 313 benchmark proves to be a significant challenge for assessing Thinking-with-Images capabilities,  
 314 even for advanced models such as o3-TU, which leverage a code interpreter.  
 315

316 **Result 2: Traditional non-agentic models perform poorly on TIR-Bench.** Across all tasks,  
 317 non-tool-using MLLMs show poor performance: the performance of most open-source models is  
 318 close to or slightly higher than the random guess performance while the top-performing MLLM,  
 319 Gemini-2.5-pro, surpasses random guess results by only 15%. These results highlight that, without  
 320 agentic tool-using abilities, MLLMs can not perform well on TIR-Bench.  
 321

322 **Result 3: Agentic tool-using is essential for TIR-Bench.** The o3-TU model (OpenAI, 2025a)  
 323 demonstrates the strongest overall performance, achieving the highest average accuracy at 46%.  
 This represents a substantial lead, outperforming the Gemini-2.5-Pro model by nearly 17% and the  
 o3 model without a code interpreter by 19%. With tool-use enabled, it achieves state-of-the-art  
 324

324 Table 2: Model Accuracy (%) Across Various Evaluation Tasks. SR: Symbolic Reasoning, WS:  
 325 Word Search, LL-VQA: Low-Light VQA, IR: Instrument Reasoning, SD: Spot Difference, JG:  
 326 Jigsaw Game, VS: Visual Search, RG: Rotation Game, Pro.: Proportion VQA. o3-TU: o3-tool-  
 327 using, i.e., o3: o3 without code interpreter.

Model	All	Color	Pro.	OCR	SR	Maze	Math	WS	LL-VQA	IR	SD	JG	VS	RG
Random Guess	13.5	28.0	6.7	-	14.0	13.3	15.8	0.0	4.0	8.8	22.6	5.8	22.5	16.0
<i>Open-Source MLLMs</i>														
DeepSeek-VL2-Direct	13.0	25.0	10.0	5.0	8.0	17.5	17.5	0.0	20.0	13.8	14.6	0.0	22.5	12.0
DeepSeek-VL2-Think	13.4	30.0	12.5	5.0	10.0	22.5	15.8	1.0	22.0	8.8	8.3	0.0	21.7	14.7
Keye-VL-8B	14.8	32.0	22.5	3.3	18.0	25.0	18.3	0.0	6.0	11.2	9.0	0.0	21.7	14.7
Phi-4-Multimodal	16.3	28.0	22.5	8.3	16.0	14.2	19.2	1.0	10.0	12.5	25.3	0.0	25.8	24.0
Qwen3-VL-8B-Instruct	16.9	30.0	10.0	41.7	14.0	30.8	18.3	2.0	20.0	16.2	9.8	0.0	22.5	14.7
Qwen3-VL-8B-Thinking	15.8	29.0	20.8	33.3	16.0	20.0	20.8	0.0	10.0	13.8	1.5	0.0	25.8	16.0
Llava-1.6-M-7B	11.3	27.0	7.5	3.3	16.0	4.2	16.7	0.0	14.0	6.3	18.0	0.0	22.5	12.0
Llava-1.6-V-7B	11.5	27.0	10.8	0.0	10.0	15.0	12.5	1.0	8.0	7.5	12.2	0.0	24.2	13.3
Llava-1.6-34B	13.0	31.0	6.7	1.7	20.0	15.8	18.3	0.0	16.0	16.3	11.9	0.0	21.7	10.7
Llava-Next-72B	11.2	20.0	15.8	3.3	8.0	10.8	15.0	0.0	10.0	11.3	16.3	0.0	23.3	12.0
Qwen2.5-VL-3B	17.7	27.0	20.0	31.7	12.0	21.7	20.8	0.0	12.0	13.8	29.7	0.0	26.7	12.0
Qwen2.5-VL-7B	16.0	21.0	10.8	48.3	14.0	15.0	24.2	0.0	22.0	11.3	24.4	0.0	21.7	9.3
Qwen2.5-VL-32B	18.7	26.0	19.2	25.0	10.0	18.3	23.3	2.0	14.0	15.0	13.1	5.4	48.3	13.3
Qwen2.5-VL-72B	19.7	37.0	15.0	33.3	24.0	35.0	22.5	3.0	32.0	12.5	14.1	0.0	25.8	12.0
InternVL3-8B	16.9	23.0	11.7	0.0	6.0	33.3	21.7	2.0	22.0	8.8	16.6	4.5	36.7	17.3
InternVL3-38B	19.1	24.0	10.8	3.3	26.0	23.3	29.2	8.0	28.0	13.8	14.6	5.1	44.2	13.3
InternVL3-78B	21.4	25.0	21.7	3.3	24.0	32.5	23.3	8.0	28.0	16.3	18.9	5.8	39.2	26.7
<i>Proprietary MLLMs</i>														
GPT-4.1	18.8	36.0	7.5	11.7	12.0	17.5	25.0	4.0	24.0	11.3	30.9	5.1	34.2	22.7
GPT-4o	17.3	26.0	22.5	10.0	10.0	20.0	15.8	0.0	26.0	7.5	19.4	6.2	35.0	20.0
Gemini-2.5-Flash	25.2	34.0	20.0	30.0	26.0	17.5	30.8	10.0	42.0	13.8	18.5	8.0	55.8	29.3
Gemini-2.5-Pro	28.9	44.0	21.7	25.0	34.0	24.2	30.8	12.0	42.0	20.0	28.5	10.4	<b>58.3</b>	30.7
Grok-4	22.5	35.0	<b>53.3</b>	6.7	20.0	25.8	19.2	2.00	22.0	12.5	27.0	10.0	25.8	18.7
o4-mini	21.2	39.0	17.5	8.3	12.0	13.3	21.7	5.0	30.0	18.8	33.0	8.0	39.2	26.7
o3	26.9	36.0	34.2	8.3	34.0	29.2	24.2	4.0	28.0	17.5	37.2	10.8	47.5	33.3
<i>Tool-Using MLLMs</i>														
Qwen2.5-VL-72B-TU	24.0	39.0	26.7	41.7	20.0	23.3	20.8	3.0	36.0	18.8	19.2	5.3	45.8	21.3
Qwen3-VL-235B-TU	24.9	48.0	20.0	48.3	20.0	17.5	22.5	11.0	32.0	17.5	22.4	7.3	43.3	25.3
DeepEyes	17.3	22.0	6.7	41.7	19.9	16.7	20.0	1.0	16.0	3.8	19.9	3.9	50.8	12.0
PyVision	31.8	53.0	26.7	<b>63.3</b>	54.0	15.8	25.8	10.0	32.0	17.5	36.4	7.6	55.0	46.7
o4-mini-TU	37.5	53.0	21.7	53.3	58.0	34.2	31.7	55.0	<b>44.0</b>	13.8	38.9	11.8	47.5	52.0
o3-TU	<b>46.0</b>	<b>55.0</b>	31.7	53.3	<b>66.0</b>	<b>42.5</b>	<b>50.0</b>	<b>64.0</b>	42.0	<b>21.3</b>	<b>41.0</b>	<b>16.4</b>	57.5	<b>77.3</b>

356 results on the majority of the tasks, winning 10 out of the total 14 categories. The o3-TU and o4-  
 357 TU models demonstrate a large performance improvement on tasks involving straightforward image  
 358 manipulation or processing, including the rotation game, rotated image OCR, and word search.  
 359 Similar phenomenon appears in PyVision, which implements thinking-with-images abilities based  
 360 on GPT-4.1. PyVision brings 13% accuracy improvement compared with GPT-4.1.

361 We also observe that, although o3-TU excels in most categories, the improvements are not uniform.  
 362 For example, for complex tasks such as *Jigsaw game*, the performance of o3-TU is still very low. On  
 363 *Proportion VQA*, performance surprisingly decreases from 34.2% to 31.7%. This task requires calling  
 364 external segmentation models such as Segment Anything (Kirillov et al., 2023b) to obtain a good  
 365 rough estimate of the object segments. However, the current o3-TU model can only write executable  
 366 code to manipulate images, but lacks the capability to call segmentation models specifically.

#### 4.3 QUALITATIVE ANALYSIS

369 We present several examples of o3-TU responses here and examples of other model responses in  
 370 Appendix G. . Since the responses from the OpenAI API contain no reasoning process, we re-ran  
 371 the questions in the web-based ChatGPT interface and analyzed the responses. Figure 4 shows an  
 372 case of instrument reading. The model repeatedly crops the region around the pointer, checks its  
 373 position, and guesses the answer (highlighted in blue). After several cycles of cropping, observing,  
 374 and reflecting, o3 finally confirms its answer as “400,” which is correct. Figure 5 shows a case of  
 375 jigsaw puzzle involved a lot of ineffective attempts. The model first divided the complete image  
 376 into segments, then tried to compare and judge similarity by “understanding” the image as a whole.  
 377 In the early empirical stage, the model made nearly 55 iterations, but failed to obtain any usable  
 378 partial results. After that, it began to use edge comparison, sampling the borders of image pieces

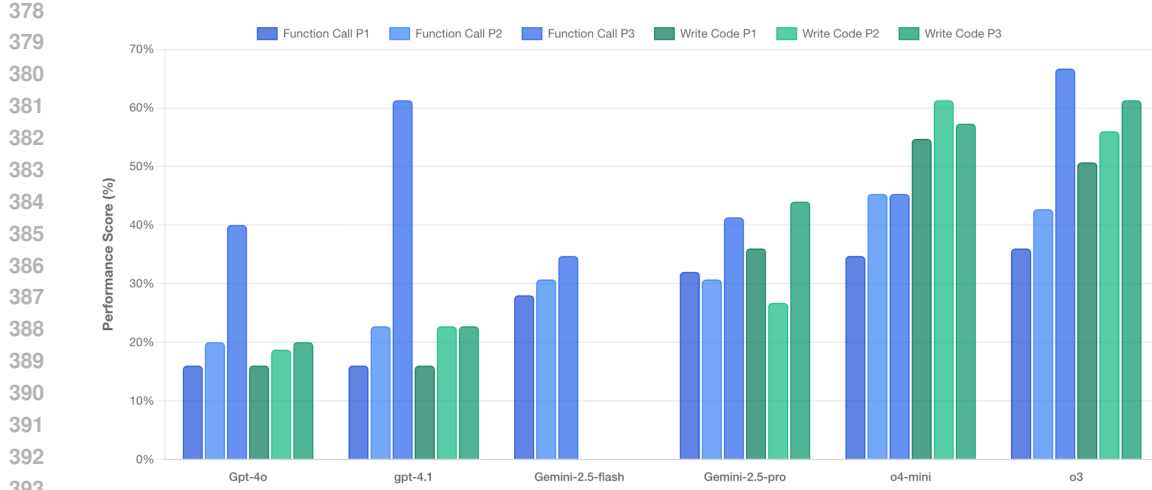


Figure 3: Comparison of function-calling and code-writing abilities across models. Function calling uses a predefined rotation function, while code writing requires the model to implement it. P1 includes only the question; P2 adds a hint to use the function; P3 explicitly instructs testing each degree in the answer choices. Stronger models (e.g., o3) perform better at code writing, whereas weaker ones (e.g., GPT-4.0) perform better at function calling.

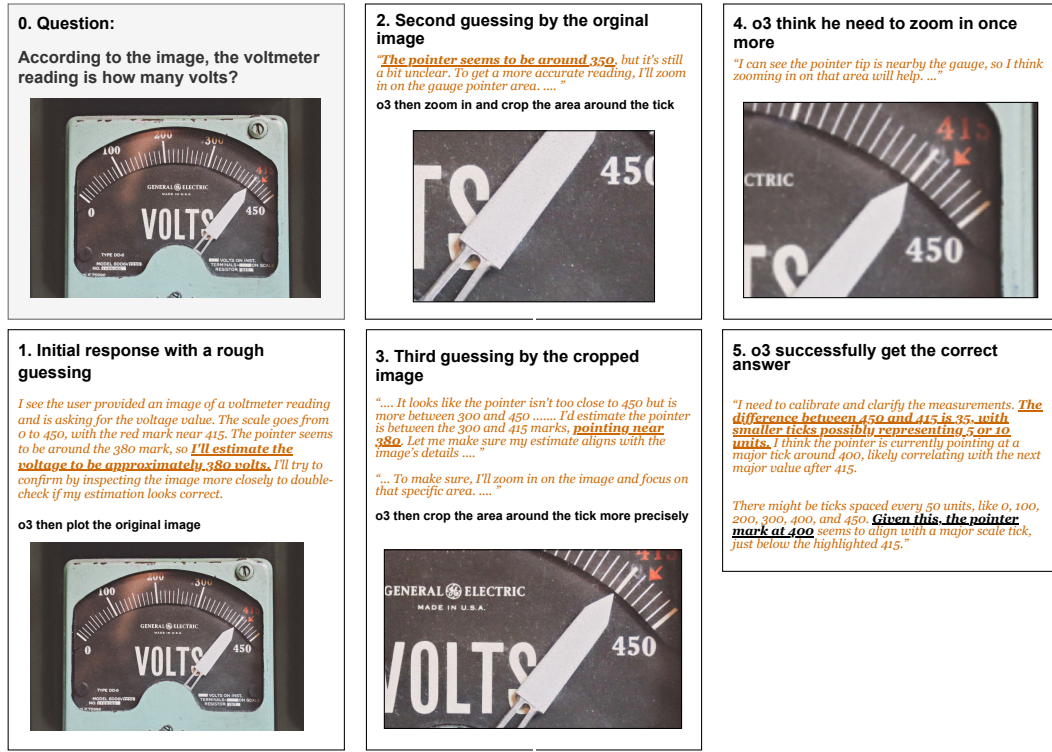


Figure 4: An example of o3 solving an case of instrument reading from TIR-Bench.

and comparing them pair by pair, which also did not produce effective outcomes. The model then started to develop algorithms, applying brute-force permutations to explore possible arrangements and calculate similarity. However, the initial algorithm did not work. After modifying the sampling method, the model, through more than 36,000 attempts, achieved a high similarity score that corresponded to the correct solution. This demonstrates that relying solely on the model’s raw visual capabilities is insufficient; only code-based perception proves to be reliable.



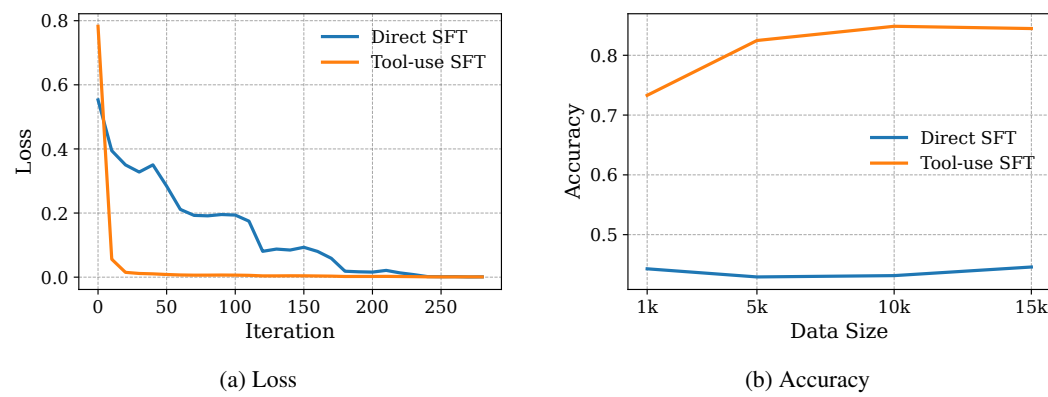


Figure 6: Comparison of change of loss and accuracy between direct SFT and tool-use SFT.

#### 4.5 FINE-TUNING COMPARISON EXPERIMENT RESULTS

In this subsection, we report the experimental results on the different fine-tuning strategies on rotated OCR task.

**Setup.** We use the rotated image OCR task as a case study to evaluate data scaling performance. We created training sets of varying sizes: 1k, 5k, 10k, and 15k samples—by randomly selecting and rotating images from the OCRDataset (Minh, 2024). We then compared two distinct training strategies: (1). Direct SFT: A standard supervised fine-tuning approach where the model is trained to map the rotated image directly to the ground-truth text. (2). Tool-Use SFT: An agentic approach where the model first learns to output the correct rotation degree. The restored image is then concatenated with the original context, and the model is subsequently trained to read the text from this corrected visual input. We use Qwen-2.5-VL-7B and fully fine-tune all parameters with 5 epochs.

**Results.** We report accuracy on the Rotated OCR task in Figure 6b and the loss curves on 15k samples in Figure 6a. Overall, Tool-use SFT significantly outperforms Direct SFT. For Tool-use SFT, performance scales positively with data size, whereas Direct SFT shows no such trend. This suggests that simply scaling data for Direct SFT is ineffective on tasks requiring image-based reasoning. We also observe that Tool-use SFT’s loss decreases much faster despite starting from a higher initial value. This is likely because Qwen-2.5-VL was not pretrained with function-calling, leading to higher initial loss. Furthermore, since Qwen-2.5-VL was trained mostly on correctly oriented OCR data, fine-tuning it directly on rotated data may cause forgetting. In contrast, restoring image orientation before text output avoids this issue, which may explain the faster loss reduction.

## 5 CONCLUSION

In this paper, we propose TIR-Bench, a comprehensive benchmark designed to evaluate the thinking-with-images ability of agentic MLLMs. TIR-Bench is composed of 13 meticulously collected tasks that assess a wide range of tool-assisted reasoning skills. By assessing diverse MLLMs on TIR-Bench, including both standard models and those augmented with tool- use capabilities, we find that TIR-Bench is a challenging benchmark for all models that necessitates thinking-with-images capabilities for successful completion. Lastly, we conduct a pilot study comparing direct and agentic fine-tuning for image-operation tasks and evaluating the function-calling abilities of various MLLMs.

## 6 LIMITATION

(1). The pilot study experiment comparing agentic SFT and directly SFT was conducted on only one task from our benchmark (Rotated-OCR). This task specifically tests an image manipulation-to-extraction pipeline. It remains an open question whether the superiority of agentic SFT would hold for the other 12 tasks in TIR-Bench. (2). We also note that some tasks, such as word search, are less common in real-world settings. We leave the inclusion of more real-world data for testing these abilities (e.g., pixel comparison) for future work.

540 REFERENCES  
541

542 Abdelrahman Abouelenin, Atabak Ashfaq, Adam Atkinson, Hany Awadalla, Nguyen Bach, Jianmin  
543 Bao, Alon Benhaim, Martin Cai, Vishrav Chaudhary, Congcong Chen, et al. Phi-4-mini technical  
544 report: Compact yet powerful multimodal language models via mixture-of-loras. *arXiv preprint*  
545 *arXiv:2503.01743*, 2025.

546 Anthropic. Introducing claude 4, 2025. URL <https://www.anthropic.com/news/claude-4>.

547 Shuai Bai, Keqin Chen, Xuejing Liu, Jialin Wang, Wenbin Ge, Sibo Song, Kai Dang, Peng Wang,  
548 Shijie Wang, Jun Tang, et al. Qwen2. 5-vl technical report. *arXiv preprint arXiv:2502.13923*,  
549 2025.

550 Google Gemini Team. Gemini 2.5: Pushing the frontier with advanced reasoning, multimodality,  
551 long context, and next generation agentic capabilities. *arXiv preprint*, (arXiv:2507.06261), 2025.

552 Yushi Hu, Weijia Shi, Xingyu Fu, Dan Roth, Mari Ostendorf, Luke Zettlemoyer, Noah A. Smith,  
553 and Ranjay Krishna. Visual sketchpad: Sketching as a visual chain of thought for multimodal  
554 language models. In *NeurIPS*, 2024.

555 Aaron Hurst and OpenAI. Gpt-4o system card. *arXiv preprint arXiv:2410.21276*, 2024. doi:  
556 10.48550/arXiv.2410.21276. URL <https://arxiv.org/abs/2410.21276>. “o” for omni  
557 — large multimodal model accepting text, audio, image, and video inputs.

558 Sahar Kazemzadeh, Vicente Ordonez, Mark Matten, and Tamara Berg. Referitgame: Referring to  
559 objects in photographs of natural scenes. In *Proceedings of the 2014 conference on empirical*  
560 *methods in natural language processing (EMNLP)*, pp. 787–798, 2014.

561 Alexander Kirillov, Eric Mintun, Nikhila Ravi, Hanzi Mao, Chloe Rolland, Laura Gustafson, Tete  
562 Xiao, Spencer Whitehead, Alexander C. Berg, Wan-Yen Lo, Piotr Dollár, and Ross Girshick.  
563 Segment anything, 2023a. URL <https://arxiv.org/abs/2304.02643>.

564 Alexander Kirillov, Eric Mintun, Nikhila Ravi, Hanzi Mao, Chloe Rolland, Laura Gustafson, Tete  
565 Xiao, Spencer Whitehead, Alexander C. Berg, Wan-Yen Lo, Piotr Dollár, and Ross Girshick.  
566 Segment anything, 2023b. URL <https://arxiv.org/abs/2304.02643>.

567 Xin Lai, Junyi Li, Wei Li, Tao Liu, Tianjian Li, and Hengshuang Zhao. Mini-o3: Scaling up  
568 reasoning patterns and interaction turns for visual search. *arXiv preprint arXiv:2509.07969*, 2025.

569 Bo Li, Yuanhan Zhang, Dong Guo, Renrui Zhang, Feng Li, Hao Zhang, Kaichen Zhang, Peiyuan  
570 Zhang, Yanwei Li, Ziwei Liu, et al. Llava-onevision: Easy visual task transfer. *arXiv preprint*  
571 *arXiv:2408.03326*, 2024a.

572 Bohao Li, Yuying Ge, Yixiao Ge, Guangzhi Wang, Rui Wang, Ruimao Zhang, and Ying Shan.  
573 Seed-bench: Benchmarking multimodal large language models. In *Proceedings of the IEEE/CVF*  
574 *Conference on Computer Vision and Pattern Recognition*, pp. 13299–13308, 2024b.

575 Kaixin Li, Yuchen Tian, Qisheng Hu, Ziyang Luo, and Jing Ma. Mmcode: Evaluating multi-  
576 modal code large language models with visually rich programming problems. *arXiv preprint*  
577 *arXiv:2404.09486*, 2024c.

578 Ming Li, Jike Zhong, Tianle Chen, Yuxiang Lai, and Konstantinos Psounis. Eee-bench: A com-  
579 prehensive multimodal electrical and electronics engineering benchmark. In *Proceedings of the*  
580 *Computer Vision and Pattern Recognition Conference*, pp. 13337–13349, 2025.

581 Yijun Liang, Ming Li, Chenrui Fan, Ziyue Li, Dang Nguyen, Kwesi Cobbina, Shweta Bhardwaj,  
582 Juhai Chen, Fuxiao Liu, and Tianyi Zhou. Colorbench: Can vlms see and understand the col-  
583 orful world? a comprehensive benchmark for color perception, reasoning, and robustness. *arXiv*  
584 *preprint arXiv:2504.10514*, 2025.

585 Haotian Liu, Chunyuan Li, Yuheng Li, and Yong Jae Lee. Improved baselines with visual instruction  
586 tuning. In *Proceedings of the IEEE/CVF conference on computer vision and pattern recognition*,  
587 pp. 26296–26306, 2024a.

594 Shilong Liu, Zhaoyang Zeng, Tianhe Ren, Feng Li, Hao Zhang, Jie Yang, Qing Jiang, Chunyuan Li,  
 595 Jianwei Yang, Hang Su, Jun Zhu, and Lei Zhang. Grounding dino: Marrying dino with grounded  
 596 pre-training for open-set object detection. In *ECCV*, 2024b.

597

598 Yuan Liu, Haodong Duan, Yuanhan Zhang, Bo Li, Songyang Zhang, Wangbo Zhao, Yike Yuan,  
 599 Jiaqi Wang, Conghui He, Ziwei Liu, et al. Mmbench: Is your multi-modal model an all-around  
 600 player? *arXiv preprint arXiv:2307.06281*, 2023.

601

602 Yuliang Liu, Zhang Li, Mingxin Huang, Biao Yang, Wenwen Yu, Chunyuan Li, Xu-Cheng Yin,  
 603 Cheng-Lin Liu, Lianwen Jin, and Xiang Bai. Ocrbench: on the hidden mystery of ocr in large  
 604 multimodal models. *Science China Information Sciences*, 67(12):220102, 2024c.

605

606 Pan Lu, Ran Gong, Shibiao Jiang, Liang Qiu, Siyuan Huang, Xiaodan Liang, and Song-Chun Zhu.  
 607 Inter-gps: Interpretable geometry problem solving with formal language and symbolic reasoning.  
 608 *arXiv preprint arXiv:2105.04165*, 2021.

609

610 Pan Lu, Hritik Bansal, Tony Xia, Jiacheng Liu, Chunyuan Li, Hannaneh Hajishirzi, Hao Cheng, Kai-  
 611 Wei Chang, Michel Galley, and Jianfeng Gao. Mathvista: Evaluating mathematical reasoning of  
 612 foundation models in visual contexts. *arXiv preprint arXiv:2310.02255*, 2023.

613

614 Minh. Combined ocr dataset. Hugging Face Datasets, 2024. URL [https://huggingface.co/datasets/ducto489/ocr\\_datasets](https://huggingface.co/datasets/ducto489/ocr_datasets).

615

616 OpenAI. Openai o3: A reasoning model trained to think before responding. Blog post / system card,  
 617 April 2025a. Introducing OpenAI o3 and o4-mini.

618

619 OpenAI. Introducing gpt-4.1 in the api, 2025b. URL <https://openai.com/index/gpt-4-1/>.

620

621 OpenAI. Thinking with images, 2025c. URL <https://openai.com/index/thinking-with-images/>.

622

623 Ji Qi, Ming Ding, Weihan Wang, Yushi Bai, Qingsong Lv, Wenyi Hong, Bin Xu, Lei Hou, Juanzi  
 624 Li, Yuxiao Dong, and Jie Tang. Cogcom: A visual language model with chain-of-manipulations  
 625 reasoning. In *ICLR*, 2025.

626

627 Runqi Qiao, Qiuna Tan, Guanting Dong, Minhui Wu, Chong Sun, Xiaoshuai Song, Zhuoma  
 628 GongQue, Shanglin Lei, Zhe Wei, MiaoXuan Zhang, et al. We-math: Does your large multi-  
 629 modal model achieve human-like mathematical reasoning? *arXiv preprint arXiv:2407.01284*,  
 630 2024.

631

632 Pooyan Rahmazadehgerwi, Logan Bolton, Mohammad Reza Taesiri, and Anh Totti Nguyen. Vision  
 633 language models are blind. In *Proceedings of the Asian Conference on Computer Vision*, pp. 18–  
 634 34, 2024.

635

636 Alex Su, Haozhe Wang, Weiming Ren, Fangzhen Lin, and Wenhui Chen. Pixel reasoner: In-  
 637 centivizing pixel-space reasoning with curiosity-driven reinforcement learning, 2025a. URL  
 638 <https://arxiv.org/abs/2505.15966>.

639

640 Zhaochen Su, Peng Xia, Hangyu Guo, Zhenhua Liu, Yan Ma, Xiaoye Qu, Jiaqi Liu, Yanshu Li,  
 641 Kaide Zeng, Zhengyuan Yang, et al. Thinking with images for multimodal reasoning: Founda-  
 642 tions, methods, and future frontiers. *arXiv preprint arXiv:2506.23918*, 2025b.

643

644 Dídac Surís, Sachit Menon, and Carl Vondrick. Vipergpt: Visual inference via python execution for  
 645 reasoning. In *ICCV*, 2023.

646

647 Kwai Keye Team, Biao Yang, Bin Wen, Changyi Liu, Chenglong Chu, Chengru Song, Chongling  
 648 Rao, Chuan Yi, Da Li, Dunju Zang, et al. Kwai keye-vl technical report. *arXiv preprint  
 649 arXiv:2507.01949*, 2025.

650

651 Qwen Team. Qwen3 technical report, 2025. URL <https://arxiv.org/abs/2505.09388>.

648 Peter Tong, Ellis Brown, Penghao Wu, Sanghyun Woo, Adithya Jairam Vedagiri IYER, Sai Charitha  
 649 Akula, Shusheng Yang, Jihan Yang, Manoj Middepogu, Ziteng Wang, et al. Cambrian-1: A fully  
 650 open, vision-centric exploration of multimodal llms. *Advances in Neural Information Processing*  
 651 *Systems*, 37:87310–87356, 2024.

652 Ke Wang, Junting Pan, Weikang Shi, Zimu Lu, Mingjie Zhan, and Hongsheng Li. Measuring multi-  
 653 modal mathematical reasoning with math-vision dataset, 2024a. URL <https://arxiv.org/abs/2402.14804>.

654 Wenbin Wang, Liang Ding, Minyan Zeng, Xiabin Zhou, Li Shen, Yong Luo, Wei Yu, and Dacheng  
 655 Tao. Divide, conquer and combine: A training-free framework for high-resolution image percep-  
 656 tion in multimodal large language models. In *Proceedings of the AAAI Conference on Artificial*  
 657 *Intelligence*, volume 39, pp. 7907–7915, 2025.

658 Xiaoxuan Wang, Ziniu Hu, Pan Lu, Yanqiao Zhu, Jieyu Zhang, Satyen Subramaniam, Arjun R  
 659 Loomba, Shichang Zhang, Yizhou Sun, and Wei Wang. Scibench: Evaluating college-level sci-  
 660 entific problem-solving abilities of large language models. *arXiv preprint arXiv:2307.10635*, 2023.

661 Zirui Wang, Mengzhou Xia, Luxi He, Howard Chen, Yitao Liu, Richard Zhu, Kaiqu Liang, Xindi  
 662 Wu, Haotian Liu, Sadhika Malladi, et al. Charxiv: Charting gaps in realistic chart understand-  
 663 ing in multimodal llms. *arXiv preprint arXiv:2406.18521*, 2024b.

664 Chen Wei, Wenjing Wang, Wenhan Yang, and Jiaying Liu. Deep retinex decomposition for low-light  
 665 enhancement. *arXiv preprint arXiv:1808.04560*, 2018.

666 Jason Wei, Xuezhi Wang, Dale Schuurmans, Maarten Bosma, Fei Xia, Ed Chi, Quoc V Le, Denny  
 667 Zhou, et al. Chain-of-thought prompting elicits reasoning in large language models. *Advances in*  
 668 *neural information processing systems*, 35:24824–24837, 2022.

669 Penghao Wu and Saining Xie. V?: Guided visual search as a core mechanism in multimodal llms.  
 670 In *Proceedings of the IEEE/CVF Conference on Computer Vision and Pattern Recognition*, pp.  
 671 13084–13094, 2024.

672 Zhiyu Wu, Xiaokang Chen, Zizheng Pan, Xingchao Liu, Wen Liu, Damai Dai, Huazuo Gao, Yiyang  
 673 Ma, Chengyue Wu, Bingxuan Wang, et al. Deepseek-vl2: Mixture-of-experts vision-language  
 674 models for advanced multimodal understanding. *arXiv preprint arXiv:2412.10302*, 2024.

675 xAI. Grok 4: Native tool use, real-time search integration, and frontier reasoning. xAI blog post /  
 676 documentation, July 2025. Includes the “Grok 4 Heavy” variant, 256 000 token context window,  
 677 and performance improvements via reinforcement learning and expanded training data.

678 Yunfei Xie, Yinsong Ma, Shiyi Lan, Alan Yuille, Junfei Xiao, and Chen Wei. Play to generalize:  
 679 Learning to reason through game play. *arXiv preprint arXiv:2506.08011*, 2025.

680 Xiang Yue, Yuansheng Ni, Kai Zhang, Tianyu Zheng, Ruoqi Liu, Ge Zhang, Samuel Stevens,  
 681 Dongfu Jiang, Weiming Ren, Yuxuan Sun, et al. Mmmu: A massive multi-discipline multi-  
 682 modal understanding and reasoning benchmark for expert agi. In *Proceedings of the IEEE/CVF*  
 683 *Conference on Computer Vision and Pattern Recognition*, pp. 9556–9567, 2024.

684 Renrui Zhang, Dongzhi Jiang, Yichi Zhang, Haokun Lin, Ziyu Guo, Pengshuo Qiu, Aojun Zhou,  
 685 Pan Lu, Kai-Wei Chang, Peng Gao, et al. Mathverse: Does your multi-modal llm truly see the  
 686 diagrams in visual math problems? *arXiv preprint arXiv:2403.14624*, 2024.

687 Xintong Zhang, Zhi Gao, Bofei Zhang, Pengxiang Li, Xiaowen Zhang, Yang Liu, Tao Yuan, Yuwei  
 688 Wu, Yunde Jia, Song-Chun Zhu, and Qing Li. Chain-of-focus: Adaptive visual search and zoom-  
 689 ing for multimodal reasoning via rl, 2025a. URL <https://arxiv.org/abs/2505.15436>.

690 Yi-Fan Zhang, Xingyu Lu, Shukang Yin, Chaoyou Fu, Wei Chen, Xiao Hu, Bin Wen, Kaiyu  
 691 Jiang, Changyi Liu, Tianke Zhang, et al. Thyme: Think beyond images. *arXiv preprint*  
 692 *arXiv:2508.11630*, 2025b.

693 Shitian Zhao, Haoquan Zhang, Shaoheng Lin, Ming Li, Qilong Wu, Kaipeng Zhang, and Chen Wei.  
 694 Pyvision: Agentic vision with dynamic tooling. *arXiv preprint arXiv:2507.07998*, 2025.

702 Ziwei Zheng, Michael Yang, Jack Hong, Chenxiao Zhao, Guohai Xu, Le Yang, Chao Shen, and  
703 Xing Yu. Deepeyes: Incentivizing “thinking with images” via reinforcement learning, 2025.  
704 URL <https://arxiv.org/abs/2505.14362>.

705

706 Zetong Zhou, Dongping Chen, Zixian Ma, Zhihan Hu, Mingyang Fu, Sinan Wang, Yao Wan,  
707 Zhou Zhao, and Ranjay Krishna. Reinforced visual perception with tools. *arXiv preprint*  
708 *arXiv:2509.01656*, 2025.

709

710 Jinguo Zhu, Weiyun Wang, Zhe Chen, Zhaoyang Liu, Shenglong Ye, Lixin Gu, Hao Tian, Yuchen  
711 Duan, Weijie Su, Jie Shao, et al. Internvl3: Exploring advanced training and test-time recipes for  
712 open-source multimodal models. *arXiv preprint arXiv:2504.10479*, 2025.

713

714

715

716

717

718

719

720

721

722

723

724

725

726

727

728

729

730

731

732

733

734

735

736

737

738

739

740

741

742

743

744

745

746

747

748

749

750

751

752

753

754

755

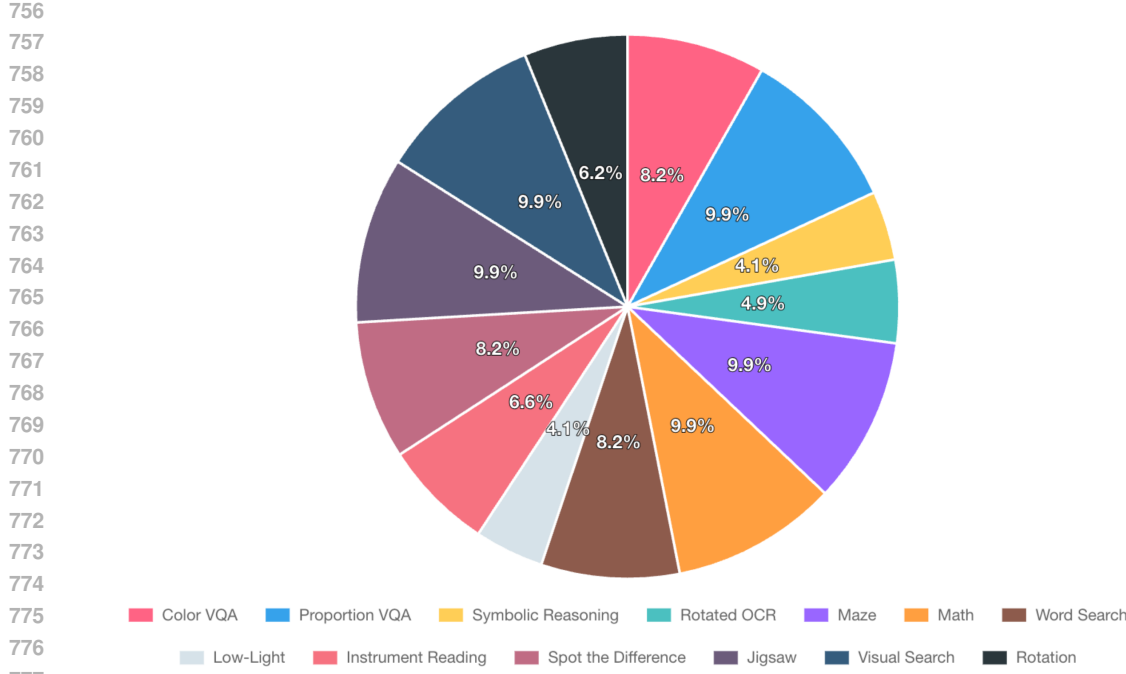


Figure 7: Task Distribution of TIR-Bench.

## A THE USE OF LARGE LANGUAGE MODELS (LLMs)

In this paper, we only used LLMs to correct the grammar and spelling errors in the writing. All the results are produced by authors.

## B DETAILED TASK DESIGN AND COLLECTION

### B.1 TASK DESIGN

To extensively validate the model’s ability to think with images we design 13 tasks. The overview of the benchmark is shown in Figure 2. We describe these 13 tasks below:

- **Color VQA task:** This task assesses the model’s ability to answer questions related to an image’s color composition. Answering these questions requires the model to programmatically process the image to obtain visual information—for instance, by writing and executing code to calculate the proportion of a specific color. The data in this task are from ColorBench Liang et al. (2025)
- **Referring Object Proportion VQA:** This task assesses the model’s agentic capabilities, requiring it to call a powerful external segmentation model to obtain an object’s mask and then programmatically calculate its proportion relative to the entire image. The images are from RefCOCO Kazemzadeh et al. (2014)
- **Rotated Image OCR:** This task evaluates a model’s ability to execute a multi-step visual reasoning process. The model must first identify that an image containing text is incorrectly oriented, then use a tool to rotate the image to its correct position, and finally perform optical character recognition (OCR) to accurately read the content. The images are from OCRBench Liu et al. (2024c).
- **Symbolic Reasoning:** This task assesses the model’s ability to apply abstract, rule-based logic to visual information. For instance, when asked to count the edges of a complex polygon, the model cannot simply guess; it must systematically identify and enumerate each distinct edge, a process that may require internal algorithms for vertex or line detection to arrive at the correct count. The data on this task are from human-annotated or Rahmazadehgervi et al. (2024)

810     • **Maze:** This task assesses the model’s ability for advanced spatial planning and algorithmic execution. The model must analyze the visual structure of the maze, devise a solution using image processing tools (such as morphological operations), and apply a pathfinding algorithm to solve it. Finally, it must draw the solution path onto the image, demonstrating its ability to translate an abstract plan into a concrete visual action. Images and questions on this task are fully synthesized.

811  
812  
813  
814  
815

816     • **Math Problems:** This task assesses the model’s ability to solve geometric problems by programmatically augmenting the visual input. To find a solution, the model must use tools to draw auxiliary constructs, such as adding lines to a diagram or imposing a coordinate system to define and calculate properties like relative lengths. Images and questions from this task are human-annotated or from MathVista Lu et al. (2023).

817  
818  
819  
820

821     • **Word Search Puzzle:** This task evaluates the model’s ability to perform fine-grained visual discrimination and anomaly detection. The image presents a field of numerous, nearly identical characters, with only a few subtle differences. Standard OCR is designed to fail in this scenario, forcing the model to devise a programmatic solution. To succeed, the model must write and execute code to perform a more fundamental analysis, such as a pixel-level comparison or a targeted visual search, to locate and identify the characters that deviate from the pattern. Images are synthesized or from free Internet platform (Wikipedia Common).

822  
823  
824  
825  
826  
827

828     • **Low-Light Image VQA:** This task evaluates the model’s ability to overcome suboptimal visual conditions. Given a low-light image where details are obscured, the model must first recognize the issue and then programmatically enhance the image, for instance, by writing and executing code to increase its contrast or brightness, before it can accurately answer questions about the content. Images are from Wei et al. (2018) and questions are annotated by humans.

829  
830  
831  
832  
833

834     • **Instrument Reading:** This task evaluates the model’s ability to perform a sequential, tool-assisted analysis. To succeed, the model must first locate the key areas for reading the instrument, then programmatically crop and enlarge these specific regions for clarity, and finally, accurately read the value from the enhanced view. Images are from Wkipedia Common and <https://unsplash.com/>, questions are annotated by humans.

835  
836  
837  
838

839     • **Spot the Difference:** This task evaluates the model’s ability to perform precise, programmatic visual comparison. To identify the differences between two nearly identical images, the model must execute a tool-based strategy, such as programmatic image subtraction, to highlight differing regions at a pixel level. After locating the discrepancies, the model must then isolate and identify the specific image patches that contain these alterations. Images are from bought spot different puzzle books.

840  
841  
842  
843  
844  
845

846     • **Jigsaw Puzzle:** This task assesses the model’s ability to perform complex spatial reasoning through an iterative, tool-based approach. The model is required to programmatically segment an image into pieces and then repeatedly attempt to reassemble them. This process involves a continuous loop of action and self-correction, where the model must evaluate each configuration to determine if the image has been successfully restored, continuing the cycle until the solution is achieved. Images are from RefCOCO Kazemzadeh et al. (2014).

847  
848  
849  
850  
851

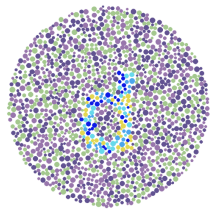
852     • **Visual Search:** This task evaluates the model’s ability to locate specific targets within a complex or high-resolution image through deep, multi-turn reasoning. To succeed, the model must engage in an iterative search process, strategically using tools to repeatedly zoom in on and analyze different regions until the object or information is found. Data are from <https://unsplash.com/>, National Gallery of Art, and HRBench Wang et al. (2025).

853  
854  
855  
856  
857

858     • **Rotation Game:** This task assesses the model’s ability to perform iterative orientation correction (Xie et al., 2025). To restore a rotated image to its upright position, the model must programmatically test various rotation angles. After each transformation, it must visually evaluate the result to determine if the orientation is correct, engaging in a trial-and-error loop of tool-based action and visual judgment until the problem is solved. Images are from CVBench Tong et al. (2024).

859  
860  
861  
862  
863

864 C DETAILED TASK EXAMPLE  
865866  
867 C.1 COLOR  
868869  
870  
871  
872  
873

			
How many colors are there in this flag? Select from the following choices. (A) 8 (B) 9 (C) 10 (D) 11c	How many colors are there in this image? Select from the following choices. (A) 7 (B) 8 (C) 9 (D) 10	Does the horizontal bar have a uniform color? Select from the following choices. (A) Hard to tell (B) Yes (C) No	What is closest to the proportion of the color green in the image? Select from the following choices. (A) 9% (B) 13% (C) 17% (D) 21%
Answer: D	Answer: D	Answer: C	Answer: B

889  
890 Figure 8: Additional example of “Color” task.  
891  
892  
893  
894895 C.2 LOW-LIGHT  
896897  
898  
899  
900

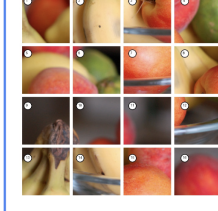
			
How many people are in the image?	How many bowls are placed vertically in the image?	How many people are in the image?	What is the most likely license plate number of the yellow car? A. 56S B. 66S C. 78S D. 89S E. 00S 9834
Answer: 5	Answer: 9	Answer: 3	Answer:

917  
918 Figure 9: Additional example of “Low-Light” task.

918 C.3 INSTRUMENT READING  
919920  
921  
922  
923  
924  
925

			
<p>Approximately what is the thermometer reading in Celsius shown in the image?</p> <p>A 37.4-37.5 B 37.5-37.6 C 37.6-37.7 D 37.7-37.8 E 37.9-38 F 38-38.1 G 38.1-38.2</p>	<p>According to the image, what is the current room temperature in Celsius as an integer?</p>	<p>What is the gauge reading in psi? Provide one decimal place (e.g., 1.1).</p>	<p>According to the thermometer in the image, approximately what is the current room temperature in Celsius?</p> <p>A 37 B 38 C 39 D 40 E 41</p>
<p>Answer: E</p>	<p>Answer: 16</p>	<p>Answer: 9</p>	<p>Answer: C</p>

941  
942 Figure 10: Additional example of “Instrument Reading” task.  
943  
944  
945  
946  
947948 C.4 JIGSAW  
949950  
951  
952  
953  
954

			
<p>Instructions: Please <u>complete</u> the jigsaw puzzle shown in the image. The original image has been divided into <math>(n) \times (n)</math> ... Question: In what order should the numbered pieces be arranged to reconstruct the original image...top to bottom). For example, 1, 16, 15, 2, 14, 8, 13, 5, 6, 7, 3, 9, 10, 11, 4, 12. Answer: [9, 1, 6, 8, 7, 2, 5, 3, 4]</p>	<p>Instructions: Please <u>complete</u> the jigsaw puzzle shown in the image. The original image has been divided into <math>(n) \times (n)</math> ... Question: In what order should the numbered pieces be arranged to reconstruct the original image...top to bottom). For example, 1, 16, 15, 2, 14, 8, 13, 5, 6, 7, 3, 9, 10, 11, 4, 12. Answer: [9, 10, 16, 11, 13, 1, 5, 6, 2, 8, 15, 4, 14, 3, 7, 12]</p>	<p>Instructions: Please <u>complete</u> the jigsaw puzzle shown in the image. The original image has been divided into <math>(n) \times (n)</math> ... Question: In what order should the numbered pieces be arranged to reconstruct the original image...top to bottom). For example, 1, 16, 15, 2, 14, 8, 13, 5, 6, 7, 3, 9, 10, 11, 4, 12. Answer: [7, 3, 1, 2, 4, 9, 5, 8, 6]</p>	<p>Instructions: Please <u>complete</u> the jigsaw puzzle shown in the image. The original image has been divided into <math>(n) \times (n)</math> ... Question: In what order should the numbered pieces be arranged to reconstruct the original image...top to bottom). For example, 1, 16, 15, 2, 14, 8, 13, 5, 6, 7, 3, 9, 10, 11, 4, 12. Answer: [7, 34, 12, 31, 33, 19, 13, 16, 28, 4, 17, 36, 30, 15, 27, 1, 2, 5, 21, 3, 22, 18, 32, 29, 35, 25, 14, 9, 11, 20, 24, 26, 6, 8, 10, 23]</p>

971 Figure 11: Additional example of “Jigsaw” task.



1026 C.7 ROTATED OCR  
1027  
1028  
1029  
1030  
1031  
1032  
1033

1034	fitnuf	1035	DOINVSDA
1036		1037	
1038	what is written in the image?	1039	what is written in the image?
1040		1041	
1042	Answer: <u>fitnuf</u>	1043	Answer: 17100
1044		1045	
1046		1047	
1048		1049	
1049	Answer: every	1050	Answer: every
1050		1051	
1051		1052	
1052		1053	
1053		1054	
1054		1055	
1055		1056	C.8 PROPORTION
1056		1057	
1057		1058	
1058		1059	
1059		1060	
1060		1061	
1061		1062	
1062		1063	
1063		1064	
1064		1065	
1065		1066	
1066		1067	
1067		1068	
1068		1069	
1069		1070	
1070		1071	
1071		1072	
1072		1073	
1073	Which of the following values is the closest to the proportion of the image occupied by right bird?\nA: 47%\nB: 39%\nC: 23%\nD: 15%\nE: 31%\nF: 7%	1074	Which of the following values is the closest to the proportion of the image occupied by man with red tie?\nA: 28%\nB: 20%\nC: 44%\nD: 36%\nE: 4%\nF: 12%
1074		1075	
1075		1076	
1076		1077	
1077		1078	
1078		1079	
1079	Answer: D	Answer: F	Answer: B
1079		1080	Answer: F

Figure 14: Additional example of “Rotated OCR” task.

1063		1064		1065		1066	
1067	Which of the following values is the closest to the proportion of the image occupied by right bird?\nA: 47%\nB: 39%\nC: 23%\nD: 15%\nE: 31%\nF: 7%	1068	Which of the following values is the closest to the proportion of the image occupied by man with red tie?\nA: 28%\nB: 20%\nC: 44%\nD: 36%\nE: 4%\nF: 12%	1069	Which of the following values is the closest to the proportion of the image occupied by right side bananas?\nA: 34%\nB: 18%\nC: 42%\nD: 2%\nE: 26%\nF: 10%	1070	Which of the following values is the closest to the proportion of the image occupied by cow on far right?\nA: 0%\nB: 16%\nC: 32%\nD: 40%\nE: 24%\nF: 8%
1071		1072		1073		1074	
1072		1073		1074		1075	
1073		1074		1075		1076	
1074		1075		1076		1077	
1075		1076		1077		1078	
1076		1077		1078		1079	
1077		1078		1079		1080	
1078		1079		1080		1081	
1079		1080		1081		1082	
1080		1081		1082		1083	
1081		1082		1083		1084	
1082		1083		1084		1085	
1083		1084		1085		1086	
1084		1085		1086		1087	
1085		1086		1087		1088	
1086		1087		1088		1089	
1087		1088		1089		1090	
1088		1089		1090		1091	
1089		1090		1091		1092	
1090		1091		1092		1093	
1091		1092		1093		1094	
1092		1093		1094		1095	
1093		1094		1095		1096	
1094		1095		1096		1097	
1095		1096		1097		1098	
1096		1097		1098		1099	
1097		1098		1099		1100	
1098		1099		1100		1101	
1099		1100		1101		1102	
1100		1101		1102		1103	
1101		1102		1103		1104	
1102		1103		1104		1105	
1103		1104		1105		1106	
1104		1105		1106		1107	
1105		1106		1107		1108	
1106		1107		1108		1109	
1107		1108		1109		1110	
1108		1109		1110		1111	
1109		1110		1111		1112	
1110		1111		1112		1113	
1111		1112		1113		1114	
1112		1113		1114		1115	
1113		1114		1115		1116	
1114		1115		1116		1117	
1115		1116		1117		1118	
1116		1117		1118		1119	
1117		1118		1119		1120	
1118		1119		1120		1121	
1119		1120		1121		1122	
1120		1121		1122		1123	
1121		1122		1123		1124	
1122		1123		1124		1125	
1123		1124		1125		1126	
1124		1125		1126		1127	
1125		1126		1127		1128	
1126		1127		1128		1129	
1127		1128		1129		1130	
1128		1129		1130		1131	
1129		1130		1131		1132	
1130		1131		1132		1133	
1131		1132		1133		1134	
1132		1133		1134		1135	
1133		1134		1135		1136	
1134		1135		1136		1137	
1135		1136		1137		1138	
1136		1137		1138		1139	
1137		1138		1139		1140	
1138		1139		1140		1141	
1139		1140		1141		1142	
1140		1141		1142		1143	
1141		1142		1143		1144	
1142		1143		1144		1145	
1143		1144		1145		1146	
1144		1145		1146		1147	
1145		1146		1147		1148	
1146		1147		1148		1149	
1147		1148		1149		1150	
1148		1149		1150		1151	
1149		1150		1151		1152	
1150		1151		1152		1153	
1151		1152		1153		1154	
1152		1153		1154		1155	
1153		1154		1155		1156	
1154		1155		1156		1157	
1155		1156		1157		1158	
1156		1157		1158		1159	
1157		1158		1159		1160	
1158		1159		1160		1161	
1159		1160		1161		1162	
1160		1161		1162		1163	
1161		1162		1163		1164	
1162		1163		1164		1165	
1163		1164		1165		1166	
1164		1165		1166		1167	
1165		1166		1167		1168	
1166		1167		1168		1169	
1167		1168		1169		1170	
1168		1169		1170		1171	
1169		1170		1171		1172	
1170		1171		1172		1173	
1171		1172		1173		1174	
1172		1173		1174		1175	
1173		1174		1175		1176	
1174		1175		1176		1177	
1175		1176		1177		1178	
1176		1177		1178		1179	
1177		1178		1179		1180	
1178		1179		1180		1181	
1179		1180		1181		1182	
1180		1181		1182		1183	
1181		1182		1183		1184	
1182		1183		1184		1185	
1183		1184		1185		1186	
1184		1185		1186		1187	
1185		1186		1187		1188	
1186		1187		1188		1189	
1187		1188		1189		1190	
1188		1189		1190		1191	
1189		1190		1191		1192	
1190		1191		1192		1193	
1191		1192		1193		1194	
1192		1193		1194		1195	
1193		1194		1195		1196	
1194		1195		1196		1197	
1195		1196		1197		1198	
1196		1197		1198		1199	
1197		1198		1199		1200	
1198		1199		1200		1201	
1199		1200		1201		1202	
1200		1201		1202		1203	
1201		1202		1203		1204	
1202		1203		1204		1205	
1203		1204		1205		1206	
1204		1205		1206		1207	
1205		1206		1207		1208	
1206		1207		1208		1209	
1207		1208		1209		1210	
1208		1209		1210		1211	
1209		1210		1211		1212	
1210		1211		1212		1213	
1211		1212		1213		1214	
1212		1213		1214		1215	
1213		1214		1215		1216	
1214		1215		1216		1217	
1215		1216		1217		1218	
1216		1217		1218		1219	
1217		1218		1219		1220	
1218		1219		1220		1221	
1219		1220		1221		1222	
1220		1221		1222		1223	
1221		1222		1223		1224	
1222		1223		1224		1225	
1223		1224		1225		1226	
1224		1225		1226		1227	
1225		1226		1227		1228	
1226		1227					

## 1080 C.9 ROTATION

1081

1082

1083

1084

1085

1086

1087

How many degrees should you rotate this image <b>CLOCKWISE</b> to restore it to its original orientation? A. 240° B. 230° C. 255° D. 235° E. 250° F. 245°	How many degrees should you rotate this image <b>CLOCKWISE</b> to restore it to its original orientation? A. 130° B. 145° C. 140° D. 150° E. 155° F. 135°	How many degrees should you rotate this image <b>CLOCKWISE</b> to restore it to its original orientation? A. 25° B. 35° C. 45° D. 15° E. 55° F. 20°	How many degrees should you rotate this image <b>CLOCKWISE</b> to restore it to its original orientation? A. 285° B. 240° C. 255° D. 270° E. 235° F. 225°
Answer: F	Answer: B	Answer: B	Answer: C

1103  
1104 Figure 16: Additional example of “Rotation” task.  
1105  
1106  
1107  
1108  
1109

## 1110 C.10 SPOT THE DIFFERENCE

1111

1112

1113

1114

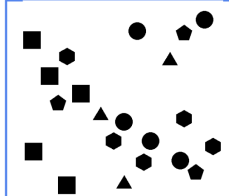
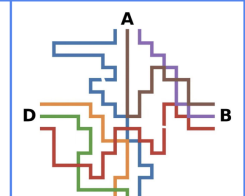
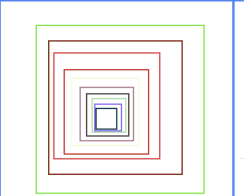
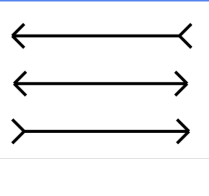
1115

1116

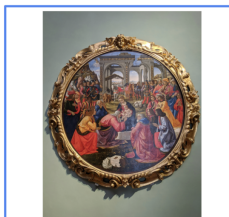
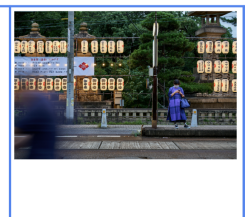
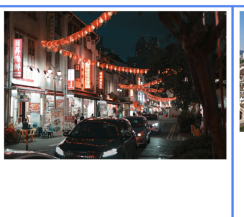
**Task Description:** Given two images of identical dimensions, each divided by thin white lines into n rows and m columns, resulting in nm small patches. ... be: ```json\n\"different_patches\": [2, 5, 6, 10]\n```\n**Problem:** Output the list of patch indices where the two images differ. Note that in this image, n is 3 and m is 4	**Task Description:** Given two images of identical dimensions, each divided by thin white lines into n rows and m columns, resulting in nm small patches. ... be: ```json\n\"different_patches\": [2, 5, 6, 10]\n```\n**Problem:** Output the list of patch indices where the two images differ. Note that in this image, n is 3 and m is 4	This is a spot-the-difference game. How many places differ between the top and bottom images?	**Task Description:** Given two images of identical dimensions, each divided by thin white lines into n rows and m columns, resulting in nm small patches. The numbering rules are as follows: 1. Patches are numbered from 1 to nm. 2. Numbering follows row-major order: the first row from left to right is 1, 2, ..., m; the first patch of the second row is m+1, and so on. The i-th...
Answer: 1, 3, 7, 8, 10, 12	Answer: 6, 8, 9, 10, 11, 12	Answer: 6	Answer: 7, 11, 12, 13, 14, 15, 19

1133  
Figure 17: Additional example of “Spot the Difference” task.

1134 C.11 SYMBOLIC REASONING  
11351136  
1137  
1138  
1139  
1140  
1141

			
<p>How many shapes are there in this image? Provide your final answer as an integer, such as 1, 2, 3.</p> <p>Answer: 21</p>	<p>How many connected single-colored paths go from A to C? A. 0 B. 1 C. 2 D. 3 E. 4</p> <p>Answer: A</p>	<p>How many nested squares are there in this image?</p> <p>A. 8 B. 10 C. 9 D. 11 E. 12</p> <p>Answer: B</p>	<p>Which of these three arrows has the longest horizontal part? A. The upper one. B. The middle one. C. The lower one.</p> <p>Answer: B</p>

1157  
1158 Figure 18: Additional example of “Symbolic Reasoning” task.  
1159  
1160  
1161  
1162  
11631164 C.12 VISUAL SEARCH  
11651166  
1167  
1168  
1169  
1170

			
<p>Q: How many colors are there in this flag? Select from the following Is a brown sheep present to the left of the central white horse? (A) 8 (B) 9 (C) 10 (D) 11</p> <p>Answer: B</p>	<p>Which lantern text listed below is furthest from the woman dressed in purple? A. The leftmost lantern labeled プリエ B. The rightmost lantern labeled 株式会社 牛長 C. The fifth lantern from the right labeled 御神燈 D. The leftmost lantern labeled 基政 E. The rightmost lantern labeled 御神燈</p> <p>Answer: B</p>	<p>目昇海鲜的服务费是多少元? 填写一个整数。</p> <p>Answer: 0</p>	<p>What is the time shown on the clock? A. Approximately 12:15 B. Approximately 11:00 C. Approximately 11:10 D. Approximately 12:00</p> <p>Answer: B</p>

1178  
1179  
1180  
1181  
1182  
1183  
1184  
1185  
1186  
1187  
1188 Figure 19: Additional example of “Visual Search” task.

1188 C.13 WORD SEARCH

1189

1190

1191

1192

1193

1194

1195

1196

1197

1198

1199

1200

1201

1202

1203

1204

1205

1206

1207

1208

1209

1210

1211

In the figure, in which row and column does the number 9 appear? The final answer should output two number list. The first number represents the row count from top to bottom, and the second number represents the column count from left to right. For example, [1, 2] means the first row and the second column	图中有多少个正字? 回答一个数字, 例如1, 2, 3。	图中入字在出现在第几行第几列? 最后答案输出两个数字, 第一个数字代表从上往下多少行, 第二个数字代表从左往右列。例如[1, 2]代表第一行第二列	How many times does the number 9 appear in this image? Answer with an integer, such as 1,2,3.
Answer: [54, 50]	Answer: 9	Answer: [31, 6]	Answer: 8

Figure 20: Additional example of “Word Search” task.

## D DETAILED PROMPTS

## D.1 WRITE CODE

prompt\_being is the prompt for the beginning turn and prompt\_return is the prompt for returning processed images to models.

Prompt strategy 1:

```
1218 prompt_1 = user_prompt
1219 prompt_2 = "The returning status and the processed image or text
1220 (if any) of the code is attached."
```

Prompt strategy 2:

```
1223 prompt_being = user_prompt + '\nPlease consider to write code to
1224 process the image.'
1225 prompt_return = 'The returning status and the processed image or
1226 text (if any) of the code is attached, you can continue to write
1227 code to process the original image for better understanding or
1228 proceed to answer the question.'
```

For prompt 3:

```
1230 prompt_1 = user_prompt + "\nPlease try to write code to rotate the
1231 original image with the rotation degree in the options to verify
1232 the correctness. You can try as many as you can."
1233
1234 prompt_2 = "The returning status and the processed image or text
1235 (if any) of the code is attached, you can continue to write code
1236 to rotate the original image with a degree of other difference
1237 options for better understanding or proceed to answer the question
1238 if you have meet the correct option."
```

## D.2 FUNCTION CALLING

For prompt strategy 1:

```

1242 prompt_1 = user_prompt
1243 prompt_2 = "The rotated image is attached."
1244
1245 For prompt strategy 2:
1246 prompt_1 = user_prompt + '\nPlease consider to call the rotation
1247 function.'
1248 prompt_2 = 'The rotated image is attached, you can continue to
1249 call the function to rotate the original image with a difference
1250 degree for better understanding or proceed to answer the
1251 question.'
1252
1253 For prompt strategy 3:
1254 prompt_1 = user_prompt + "\nPlease try to call the rotation
1255 function with the rotation degree in the options to verify the
1256 correctness. You can try as many as you can."
1257 prompt_2 = "The rotated image is attached, you can continue to
1258 call the function to rotate the original image with a degree of
1259 other difference options for better understanding or proceed to
1260 answer the question if you have meet the correct option."
1261
1262 Table 3: Average number of function calling across different prompt strategies and calling stratiefies.
1263
1264
1265
1266
1267
1268
1269
1270
1271
1272
1273
1274
1275
1276
1277
1278
1279
1280
1281
1282
1283
1284
1285
1286
1287
1288
1289
1290
1291
1292
1293
1294
1295

```

Table 3: Average number of function calling across different prompt strategies and calling stratiefies.

Model	Function			Write Code		
	Prompt 1	Prompt 2	Prompt 3	Prompt 1	Prompt 2	Prompt 3
GPT-4.1	0.00	1.15	4.68	1.32	1.68	3.95
GPT-4o	0.00	1.12	4.29	2.15	1.87	4.07
Gemini-2.5-flash	0.64	1.05	1.73	-	-	-
Gemini-2.5-pro	0.75	0.87	1.09	0.25	0.28	0.21
o4-mini	0.07	1.52	2.87	3.43	3.68	2.68
o3	0.33	1.57	3.59	6.05	5.77	5.76

## E IMPLEMENTATION DETAILS

We conduct all evaluations in zero-shot manner for fair comparison and better generalization. For open models, all experiments are done on NVIDIA A100 GPUs. For proprietary models, we use the official API. We set do sample = False, temperature = 0, max new tokens = 2048 for all open models.

## F MORE EXPERIMENTAL RESTULS

In this section, we discuss the results from synthetic data and human-annotated data. The results are shown in Table 4. First, models across all categories—from open-source to proprietary—consistently find Synthetic tasks more challenging than Annotated tasks. The average accuracy for Synthetic tasks (e.g., Maze, Jigsaw, Word Search) is significantly lower than for Annotated tasks (e.g., Color, Math, OCR). This suggests that current MLLMs struggle more with abstract spatial and logical reasoning than with recognition-based problems.

Second, the integration of tools provides a dramatic performance boost, especially for the difficult Synthetic tasks. The tool-using models, particularly o3-TU, dominate the benchmark. For example, o3-TU (43.1% Synthetic) achieves nearly double the synthetic-task accuracy of its non-tool-using counterpart, o3 (22.1%). This highlights that a tool-augmented architecture is critical for tackling these complex reasoning challenges.

Table 4: Model Accuracy (%) on Synthetic and Annotated data

Model	Synthetic Acc. (%)	Hand-Annotated Acc. (%)
Random Guess	8.0	18.2
<i>Open-Source MLLMs</i>		
Llava-1.6-M-7B	4.3	16.8
Llava-1.6-V-7B	7.8	14.4
Llava-1.6-34B	6.5	18.1
Llava-Next-72B	7.6	15.0
Qwen2.5-VL-3B	11.0	22.9
Qwen2.5-VL-7B	7.1	23.0
Qwen2.5-VL-32B	11.9	24.1
Qwen2.5-VL-72B	13.5	24.6
InternVL3-8B	13.9	19.2
InternVL3-38B	12.2	24.5
InternVL3-78B	18.7	23.5
<i>Proprietary MLLMs</i>		
GPT-4.1	10.7	25.3
GPT-4o	13.7	20.1
Gemini-2.5-Flash	16.2	32.3
Gemini-2.5-Pro	19.2	36.5
Grok-4	23.0	22.2
o4-mini	13.4	27.4
o3	22.1	30.8
<i>Tool-Using MLLMs</i>		
DeepEyes	8.0	25.4
PyVision	19.7	41.4
o4-mini-TU	32.8	41.3
o3-TU	43.1	48.2

## G EXAMPLES OF MODEL RESPONSES

In this section, we provide the response of different models.

## H ERROR ANALYSIS

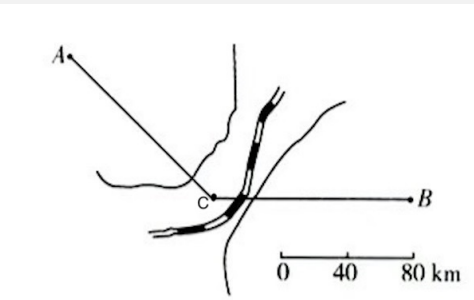
We found that approximately 37% of PyVision’s erroneous responses stem from perception errors, such as cropping incorrect image patches or misinterpreting visual content. For example, in visual search and instrument-reading tasks, PyVision may crop the wrong regions or misread instrument values. Another 61% arise from tool-generation and reasoning errors, including language-reasoning mistakes and flawed logic when generating code for image processing (e.g., producing tools that fail to solve the target problem). For instance, in jigsaw tasks, PyVision may incorrectly split the image into patches or rearrange the patches only once, resulting in wrong answers. The remaining 2

## I SUMMARY OF PYVISION RESPONSE TOOL USAGE

Because the OpenAI API does not provide intermediate reasoning or code, we have summarized the Pyvision model’s tool usage. We use GPT-4o to summarize and extract the tool of generated code. We describe these 13 tasks below:

- **Color VQA task:** pixel color counting, pixel searching, color thresholding, crop, drawing color channel histogram, image enhancement, converts an image to grayscale, color proportion calculation, pixel color analysis.

1350  
1351  
1352  
1353  
1354  
1355  
1356  
1357  
1358  
1359  
1360



1361 **Question:** Measure the distances of AC and CB according to the scale. Driving from point  
1362 A to point C and then from point C to point B, with a speed of 60 km/h, how many hours  
1363 are needed? Answer with a single number, such as 1, 2, 3.

1364 **Ground Truth: 4.**

1365 **Response from o3-TU: 4**

1366 **Response from o3: 3.**

1367 **Response from o4-mini-TU: 3**

1368 **Response from o4-mini: 2**

1369 **Response from Gemini-2.5-Pro:** By measuring the distances using the provided scale, we  
1370 find that the line segment CB is equal in length to the scale bar representing 80 km, so  
1371 Distance CB = 80 km. The segment AC is shorter than the full 80 km scale; it appears to  
1372 be three-quarters of the scale, giving Distance AC =  $0.75 \times 80 = 60$  km, or equivalently,  
1373 1.5 times the 0–40 km portion of the scale, which also gives 60 km. Therefore, the total  
1374 distance is Total Distance = Distance AC + Distance CB =  $60 + 80 = 140$  km. Assuming  
1375 a driving speed of 60 km/h, the time needed is Time =  $\frac{\text{Total Distance}}{\text{Speed}} = \frac{140}{60} \approx 2.33$  hours,  
1376 which rounded to the nearest whole number gives 2 hours.

1377 **Response from Gemini-2.5-flash:** To solve this problem, we first determine the map  
1378 scale: the scale bar shows that 223 pixels correspond to 80 km, so 1 pixel  $\approx 0.3587$  km.  
1379 The pixel coordinates are A(112, 102), C(352, 417), and B(686, 417). Using the  
1380 distance formula, the pixel length of AC is  $\sqrt{(352 - 112)^2 + (417 - 102)^2} \approx 396.01$  pixels,  
1381 and CB is  $\sqrt{(686 - 352)^2 + (417 - 417)^2} = 334$  pixels. Converting to kilometers,  
1382  $AC = 396.01 \times \frac{80}{223} \approx 142.06$  km and  $CB = 334 \times \frac{80}{223} \approx 119.82$  km. Thus, the total  
1383 distance is  $142.06 + 119.82 = 261.88$  km. With a driving speed of 60 km/h, the travel time  
1384 is  $\frac{261.88}{60} \approx 4.36$  hours, which rounds to 4 hours. Therefore, the final answer is 4.

1385  
1386

- **Referring Object Proportion VQA:** Color-Channel Histogram Drawing, crop, display image with scale guide line, Color Space Conversion, Color Thresholding, Mask Visualization, Mask Proportion Calculation, Drawing a Bounding Box,
- **Rotated Image OCR:** Image Rotation, Image Display, Enhances the contrast of an image.
- **Symbolic Reasoning:** Cropping, Zooming into Regions, Pixel color analysis, Grayscale Conversion, Edge Detection, Pixel Thresholding, Corner Detection, Pixel Counting, Contour Detection, Pixel Value Plotting, Grid Line Detection.
- **Maze:** Crop, Image display with scale guide line, pixel color counting, pixel searching, drawing points.
- **Math Problems:** Color Thresholding, Cropping, Pixel Counting, Ratio Calculation, Pixel Color Counting, Marks specific points on the image, Drawing lines, Zooming, Plotting Color Channels, Image display with scale guide line, Drawing a Rectangle, Displaying with a Scale Guide.
- **Word Search Puzzle:** Cropping, Text Extraction via OCR, pixel comparison, horizontal and vertical pixel projections, Converts the image to grayscale, Pixel Value Inspection, Two Images Difference Calculation, Pixel Peak Detection, Pixel Intensity Summation, Outlier Detection.
- **Low-Light Image VQA:** Cropping, Image Brightness and Contrast Enhancement, Image Displaying, Zooming.

1404

1405

1406

1407

1408

1409

1410

1411

1412

1413

1414

1415

1416

1417

1418

1419

1420

1421

1422

1423

1424

1425

1426

1427

1428

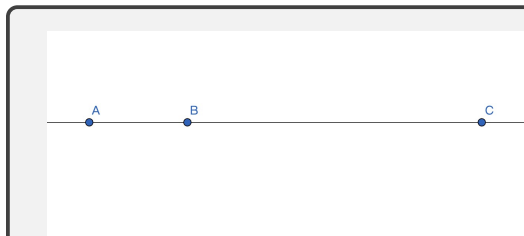
1429

1430

1431

1432

1433



**Question:** If the length of AB is 1, what is the length of BC? Provide your answer as an integer.

**Ground Truth:** 3.

**Response from o3-TU:** 3

**Response from o3:** 2.

**Response from o4-mini-TU:** From the picture the segment BC is three times as long as AB. Hence if AB = 1 then BC = 3.

**Response from o4-mini:** 8

**Response from Gemini-2.5-Pro:** Based on the visual representation of the line segments, the length of segment BC is twice the length of segment AB. Given that  $|AB| = 1$ , we calculate:

$$|BC| = 2 \times |AB| = 2 \times 1 = 2.$$

The final answer is

2

**Response from Gemini-2.5-flash:** We are given that the length of segment AB is 1. From the visual representation, it is clear that  $|AB| \approx |BC|$ . Therefore, if  $|AB| = 1$ , then  $|BC| = 1$ . The final answer is

1

Figure 21: Examples of model responses.

- **Instrument Reading:** Cropping, Displaying, Zooming.
- **Spot the Difference:** Patch Division, Image Patch Comparison, Difference Detection, Image Splitting, Cropping, Image and Pixel Thresholding, Image Displaying.
- **Jigsaw Puzzle:** Cropping, Image Displaying, Image Patch Rearranging or Reconstruction.
- **Visual Search:** Cropping, Displaying, Zooming, Contrast Enhancement.
- **Rotation Game:** Image Rotation, Image displaying, Cropping, Drawing Reference Line, Grayscale Conversion, Pixel Thresholding, Principal Component Analysis (PCA), Angle Calculation.

## J EFFICIENCY ANALYSIS

We further investigate the efficiency of the agentic framework by analyzing the **number of interaction turns** across tasks. The result of the number of interaction turns for PyVision models is shown in Figure 26. On average, PyVision requires **4.72** turns per problem to arrive at a solution. However, a detailed breakdown reveals an inverse correlation between interaction length and task success. For tasks where the model demonstrates mastery, the reasoning process is decisive and efficient: **Rotated OCR** and **Color VQA** require only **3.12** and **3.23** turns respectively, yet achieve state-of-the-art accuracies of 63.3% and 53.0%. In contrast, tasks with the highest interaction overhead often signal ineffective reasoning or error loops rather than successful deep thinking. The **Maze** and **Word Search** tasks incur the highest computational costs—averaging **8.58** and **7.34** turns—but yield the lowest performance (15.8% and 10.0%). This indicates that while the agentic loop allows for self-correction, prolonged interactions (exceeding  $\sim 5$  turns) often reflect the model struggling to find a valid solution path.

1458  
 1459  
 1460  
 1461  
 1462  
 1463  
 1464  
 1465  
 1466  
 1467  
 1468  
 1469  
 1470  
 1471  
 1472  
 1473  
 1474  
 1475  
 1476  
 1477  
 1478  
 1479  
 1480  
 1481  
 1482

1483 **Question:** How many times does the number 6 appear in this image? Answer with an  
 1484 integer, such as 1,2,3.

1485 **Ground Truth:** 4.

1486 **Response from o3-TU:** 4

1487 **Response from o3:** 10

1488 **Response from o4-mini-TU:** 4

1489 **Response from o4-mini:** 2

1490 **Response from Gemini-2.5-Pro:** 8

1491 **Response from Gemini-2.5-flash:** Let's carefully examine the image to count the occurrences of the number 6.

1492 Scanning the original image row by row: 1. Row 1: All 5s. 2. Row 2: All 5s. 3. Row 3:  
 1493 All 5s. 4. Row 4: All 5s. 5. Row 5: All 5s. 6. Row 6: 5555\*\*6\*\*5555555555 (Found 1  
 1494 '6') 7. Row 7: All 5s. 8. Row 8: All 5s. 9. Row 9: All 5s. 10. Row 10: All 5s. 11. Row  
 1495 11: 55555\*\*6\*\*5555555555 (Found 1 '6') 12. Row 12: All 5s. 13. Row 13: All 5s. 14.  
 1496 Row 14: All 5s. 15. Row 15: All 5s. 16. Row 16: 5\*\*6\*\*55555555555555 (Found 1 '6')  
 1497 17. Row 17: All 5s. 18. Row 18: All 5s. 19. Row 19: All 5s. 20. Row 20: All 5s.

1498 By carefully checking all rows, we find three instances of the number 6. The provided crops  
 1499 also highlight these same three instances.

1500 The total number of times the number 6 appears in the image is 3.

1501  
 1502  
 1503  
 1504  
 1505  
 1506  
 1507  
 1508  
 1509  
 1510  
 1511

Figure 22: Examples of model responses.



1566  
1567  
1568  
1569  
1570  
1571  
1572  
1573  
1574  
1575  
1576  
1577  
1578  
1579  
1580  
1581  
1582  
1583  
1584  
1585  
1586  
1587  
1588  
1589  
1590  
1591  
1592  
1593  
1594  
1595  
1596  
1597  
1598  
1599  
1600  
1601  
1602  
1603  
1604  
1605  
1606  
1607  
1608  
1609  
1610  
1611  
1612  
1613  
1614  
1615  
1616  
1617  
1618  
1619

**0. Question:**  
What is closest to the proportion of the color azure in the image? Select from the following  
(A) 20% (B) 30% (C) 40% (D) 50%



**1. Azure colors are defined by the threshold of the RGB channel**  
... I'll define a condition where the blue channel is greater than 150 and the red channel is below 50, which could signify azure. ...

**Write code to calculate Azure percentage using defined thresholds.**

**2. Calculate Azure percentage using defined thresholds**  
blue\_mask = (arr[:, :, 2] > 150) & (arr[:, :, 0] < 50)  
azure\_pixels = np.sum(blue\_mask)  
total\_pixels = arr.shape[0]\*arr.shape[1]  
azure\_prop = azure\_pixels / total\_pixels  
azure\_prop

**4. Execution Results**  
0.34511009720293595

**5. Adjust the defined thresholds of the RGB channel**  
... thresholds might slightly vary—including edges in the analysis—so I'll consider adjusting the threshold a bit to account for minor variations. ...

**6. Calculate Azure percentage using adjusted thresholds**  
blue\_mask2 = (arr[:, :, 2] > 120) & (arr[:, :, 0] < 100)  
azure\_prop2 = np.sum(blue\_mask2) / total\_pixels  
azure\_prop2

**7. Execution Results**  
0.3684784764927594

**8. The proportion of azure is determined by subtracting the proportion of white from the total.**  
... To refine, I could define an "azure" pixel as one with a blue hue, excluding white (defined by RGB values >= 240 across all channels). I'll count non-white pixels and see if this helps clarify how to set the threshold ...

**9. Calculate Azure percentage using adjusted thresholds**  
white\_mask = (arr[:, :, 0] > 240) /  
& (arr[:, :, 1] > 240) /  
& (arr[:, :, 2] > 240)  
nonwhite\_pixels = total\_pixels - np.sum(white\_mask)  
nonwhite\_prop = nonwhite\_pixels / total\_pixels  
nonwhite\_prop

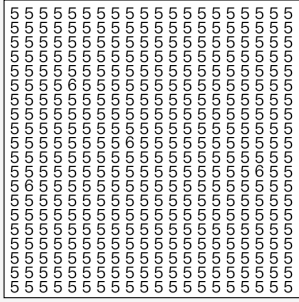
**10. Execution Results**  
0.4222376512596707

**11. Answer:**  
The azure (blue) stripes occupy a bit under half of the image—roughly four-tenths of the total pixels—so the closest option is (C) 40 %.

Figure 24: Response from o3, case a proportion estimation from TIR-Bench.

1596  
1597  
1598  
1599  
1600  
1601  
1602  
1603  
1604  
1605  
1606  
1607  
1608  
1609  
1610  
1611  
1612  
1613  
1614  
1615  
1616  
1617  
1618  
1619

**0. Question:**  
How many times does the number 6 appear in this image? Answer with an integer, such as 1,2,3.



**1. Understanding the question**  
I'm thinking of using a method in Python to analyze glyphs, where I compare a grid of glyphs to a template of "6". I'll start by segmenting the grid and determining how many columns there are, assuming a 540px width and a 30px per glyph, so probably 18 columns. I'll use this template from the first cell, and then I'll compute differences between each cell and the template. If the difference is above a threshold, I'll label it as a "6". Let's test this out!

**Few wrong step with wrong answer or meeting errors, for assuming wrong numbers of columns ....**

**2. Classify numbers by calculating differences between first glyph as template and others**  
I'm working with a 20x20 grid of glyphs, each about 12px wide and 30px high. I'll use a template of "6" and compare it against the others. To find matching cells, I'll extract the average image for the first cell and check the difference using XOR calculations, since I can't simply subtract the values. If the difference exceeds a threshold, I'll mark cells as "6". Time to implement this logic and see if it works!

**3. Check the differences**  
diffs = []  
for cell in cells:  
 h, w = cell.shape  
 new=np.zeros\_like(template)  
 new[:h,:w]=cell  
 diff = np.logical\_xor(new,template).sum()  
 diff.append(diff)  
 min(diffs), max(diffs)

**4. Execution Results**  
(0, 69)

**5. Check the distribution of differences**  
When the difference exceeds a threshold, a cell will be marked as "6". I'll check the distribution of differences to ensure accuracy. Time to implement!

**6. Check the distribution of differences**  
counts = {}  
for d in diffs:  
 counts[d] = counts.get(d, 0) + 1  
sorted\_counts = sorted(counts.items(),  
 key=lambda x: x[1],  
 reverse=True)  
sorted\_counts[:10], len(diffs)

**7. Execution Results**  
([(0, 396), (69, 4)], 400)

**8. Answer**  
4

Figure 25: Response from o3, case a word searching from TIR-Bench.

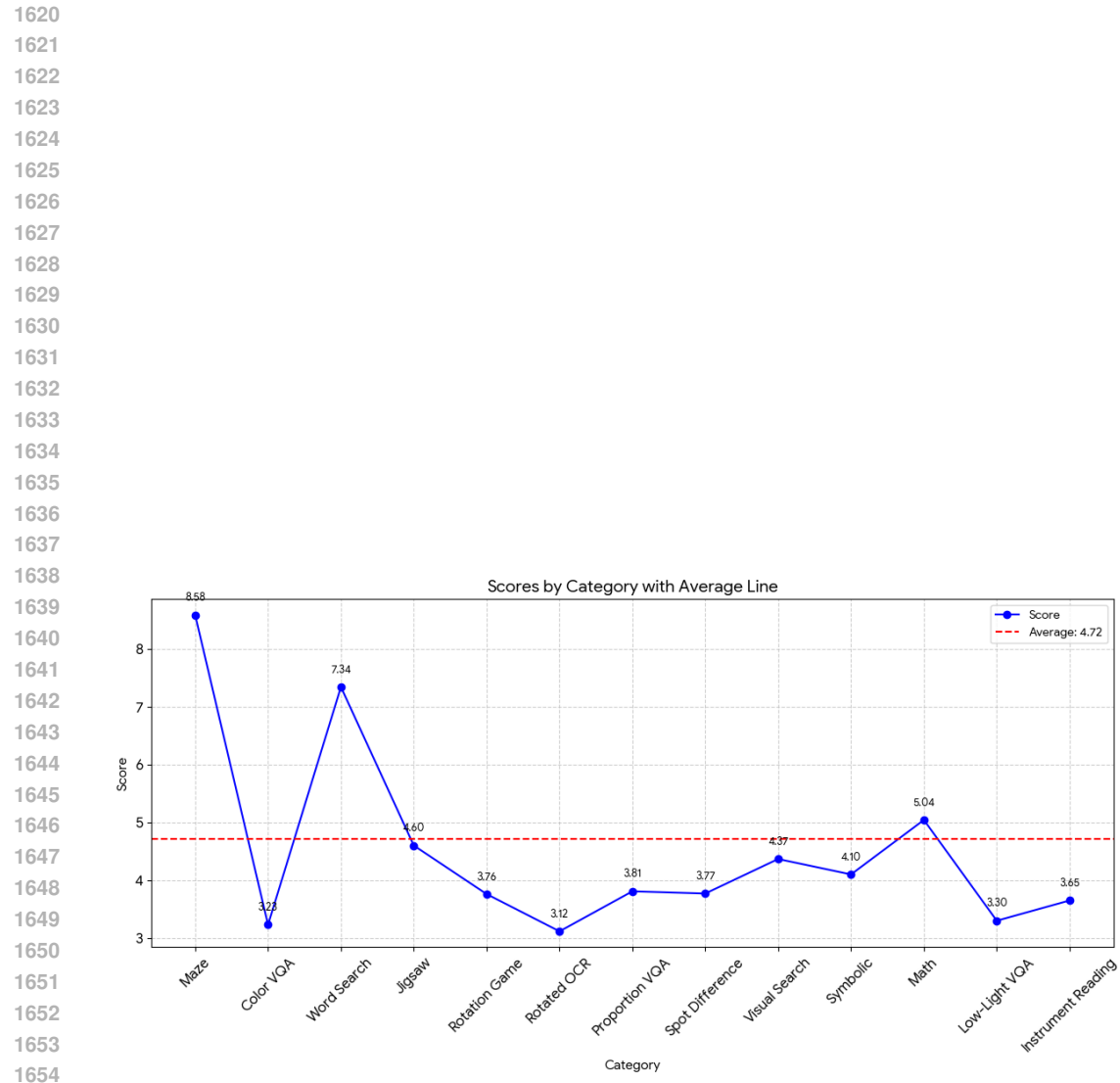


Figure 26: Number of interaction turns for the PyVision model.